

Collaborative Fluid Dynamics Research: Porous Media, Microfluidics, and Bio-Flows

***OU Supercomputing Symposium
Oct. 7, 2009***

Willy Duffle, Jesse Haubrich, Chris Kiser, Grant Armstrong,
Andrew Baker, Daniel Atkinson, Andrew Henderson, Lamar
Williams, Tim Handy, and Evan Lemley

***Department of Engineering and Physics
University of Central Oklahoma***

Dimitrios Papavassiliou, Henry Neeman, Ed O'Rear
University of Oklahoma

Four horizontal bars of varying lengths and colors (orange, grey, orange, grey) are positioned at the bottom left of the slide.

Overview

Background

Simulations

- Flow Through Porous Media (FTPM)

- Flow in Junctions/Microjunctions

- Microelbows

- Entrance Length in Microtubes

Experimental

- Millijunctions

- Bio-Scaffolds

- Renal Artery Aneurysm

- Microtubes

Future Directions

Three horizontal bars at the bottom of the slide: a thick orange bar, a medium grey bar, and a thin orange bar.

Applications

Flow in microfluidic flow networks and flow in porous networks are of interest in many engineering applications.

Applications include porous media, micro-power generation, biomedical, computer chips, chemical separation processes, micro-valves, micro-pumps, and micro-flow sensors

Yanuka, M., Dullien, F.A.L., and D.E. Elrick, 1986, "Percolation Processes And Porous Media I. Geometrical And Topological Model Of Porous Media Using A Three-Dimensional Joint Pore Size Distribution," J.Colloid Interface Sci., **112**, pp. 24-41.

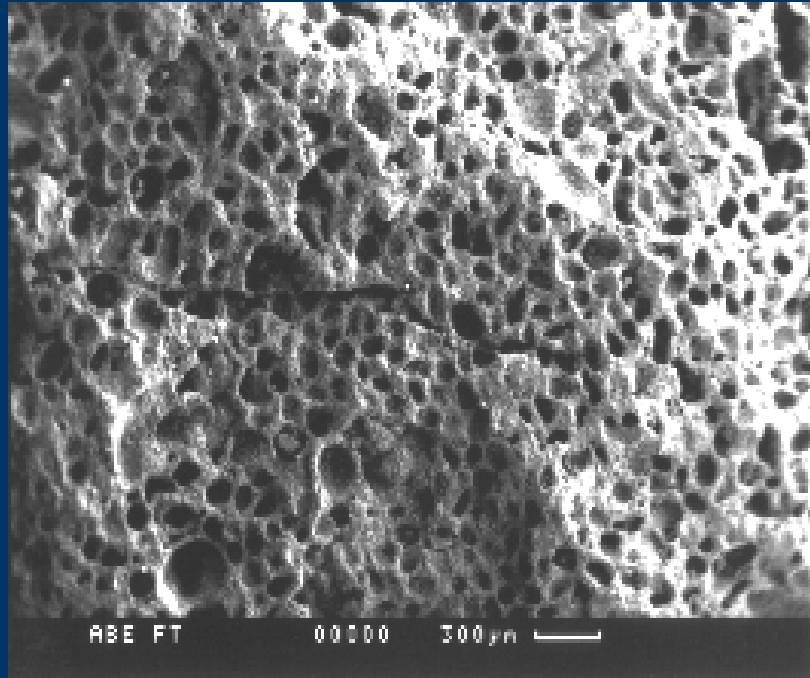
Lee, W.Y., Wong, M., and Zohar, Y., 2002, "Microchannels in Series Connected Via a Contraction/expansion Section", J. Fluid Mech., **459**, pp.187-206.

Judy, J., Maynes, D., and Webb, B.W., 2002, "Characterization of Frictional Pressure Drop for Liquid Flows Through Microchannels," Intl. J. Heat Mass Trans., **45**, pp.3477-3489.

Flow in these applications is usually laminar

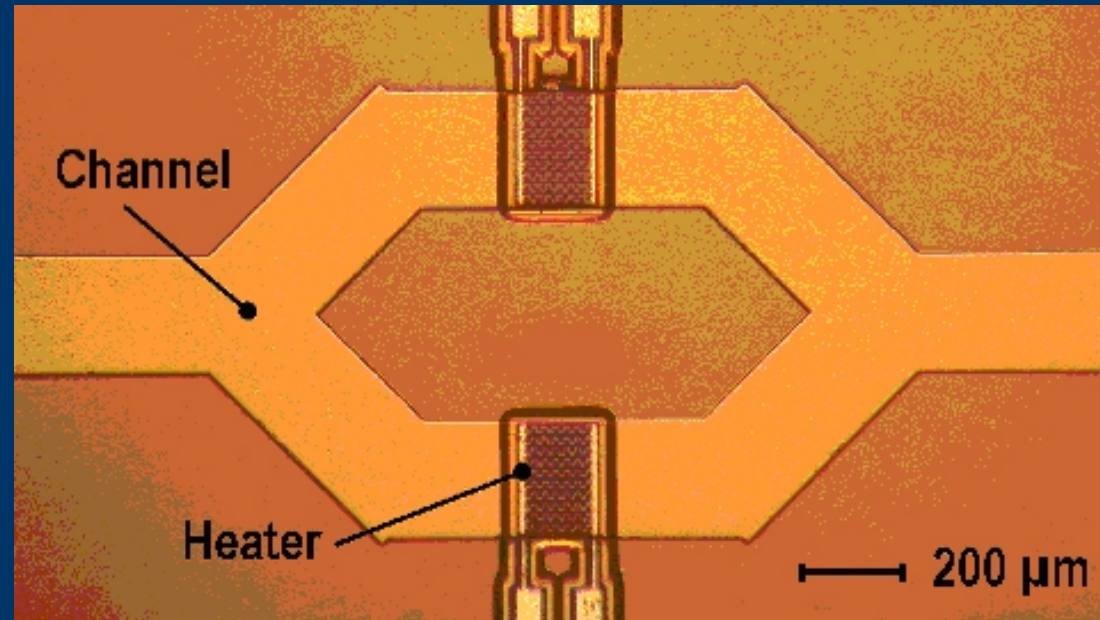
Graveson, P., Branbjerg, J., and Jensen, O.S., 1993, "Microfluidics a Review," J. Micromech. Microeng., **3**, pp.168-182.

Porous Media



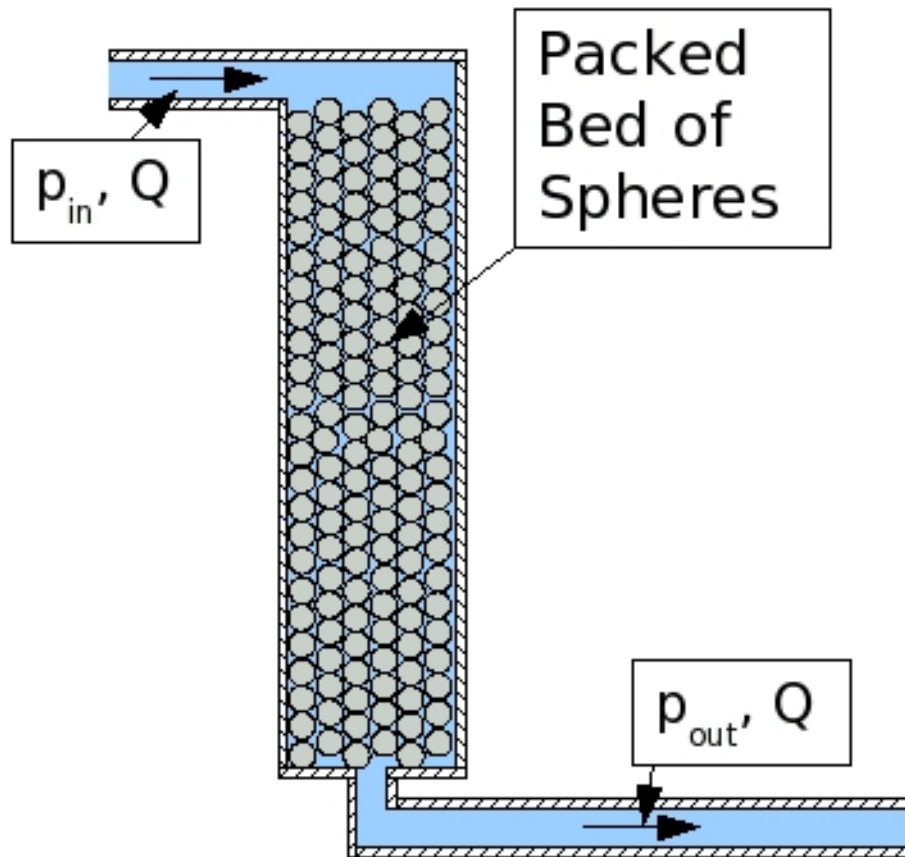
Highly porous magnesian limestone.
(www.dawntnicholson.org.uk)

Microfluidic Devices



Microfluidic Valve Structure.
(<http://www.cchem.berkeley.edu/sjmgrp/people/boris/boris.htm>)

Artificial Porous Media



Packed Beds, Gas and
Liquid Filters

Sphere sizes μm to
 cm

Hold-up for chemical
reaction, thermal
processing, or filtering

Basics of Porous Media

Low Speed Flow – Darcy's Law

$$\frac{\phi}{\alpha} = \frac{\mu}{\kappa} u$$

$p = \text{pressure}$ $x = \text{position}$
 $\mu = \text{viscosity}$ $\kappa = \text{permeability}$
 $u = \text{filtration velocity}$

High Speed Flow – Forchheimer's Law

$$\frac{\phi}{\alpha} = \frac{\mu}{\kappa} u + \rho \beta u^2$$

$\rho = \text{density}$
 $\beta = \text{Forchheimer's Coefficient}$

Packed Beds – Ergun's Equation (empirical)

$$\frac{-\Delta p}{\Delta L} = \frac{150}{d_p^2} \frac{\mu (1-\phi)^2}{\phi^3} u + \frac{175}{d_p \phi^3} \rho u^2$$

$\phi = \text{porosity}$
 $d_p = \text{mean sphere diameter}$

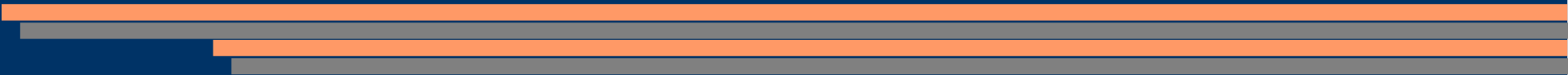
Flow Through Porous Media

Collaborative Effort with Dimitrios Papavassiliou and Henry Neeman from OU (began Fall 2004)

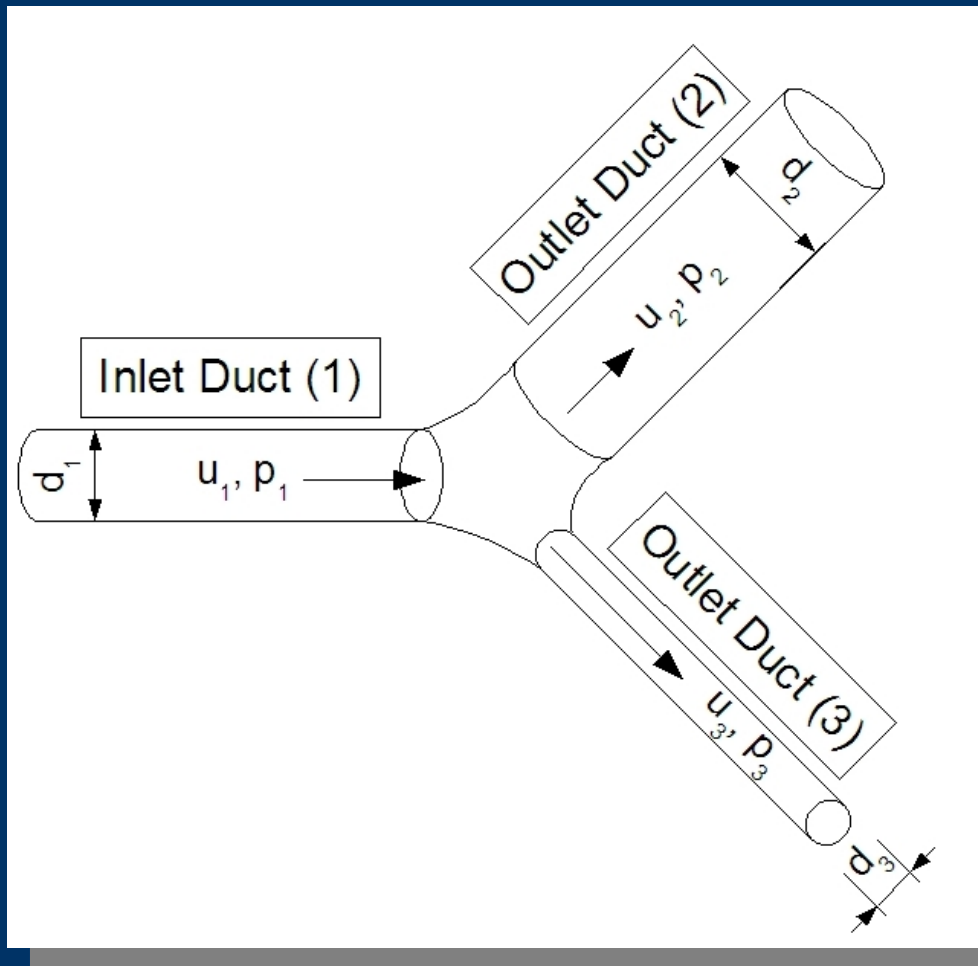
Simulation of Flow of Fluids through Porous Media

Code FTPM – Flow Through Porous Media.

Solves for velocity and pressure at pore junctions in a randomly generated pore network.

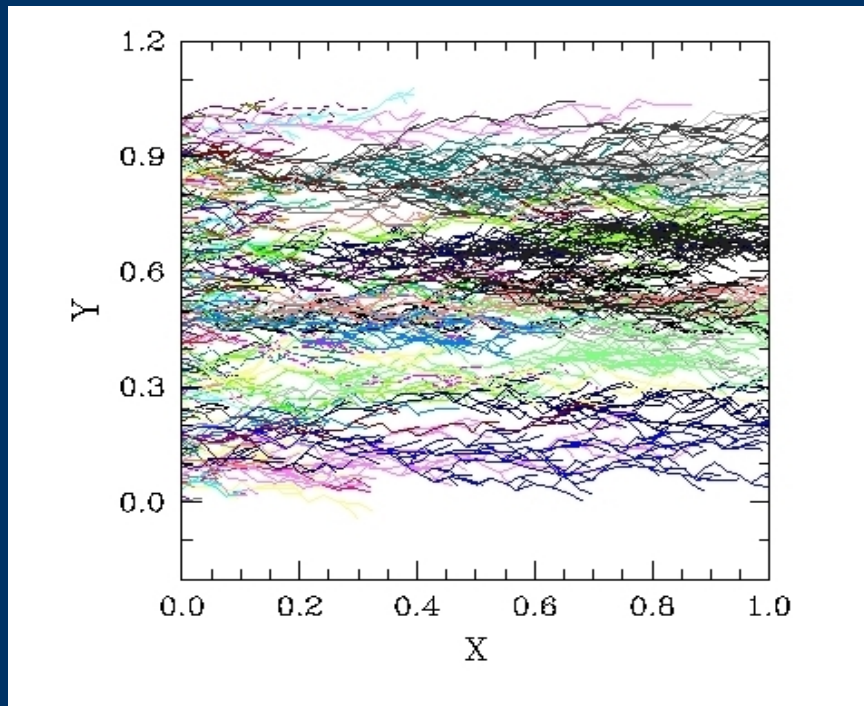


Flow Network Analysis



Design and Analysis of networks depends on knowledge of flow and energy losses in arbitrary branches. No systematic studies to generalize these bifurcations

Porous Network Simulator (Collaboration with Univ. of Oklahoma)

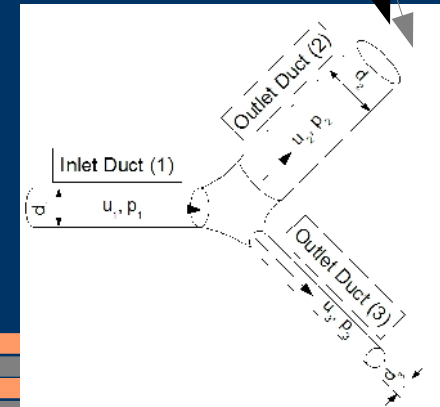


Projection on the xy plane of a 3D network that has 200 entry points at $x=0$, porosity equal to 10% and a range of $\pm 60^\circ$ relative to the x axis and $\pm 30^\circ$ relative to the y axis.

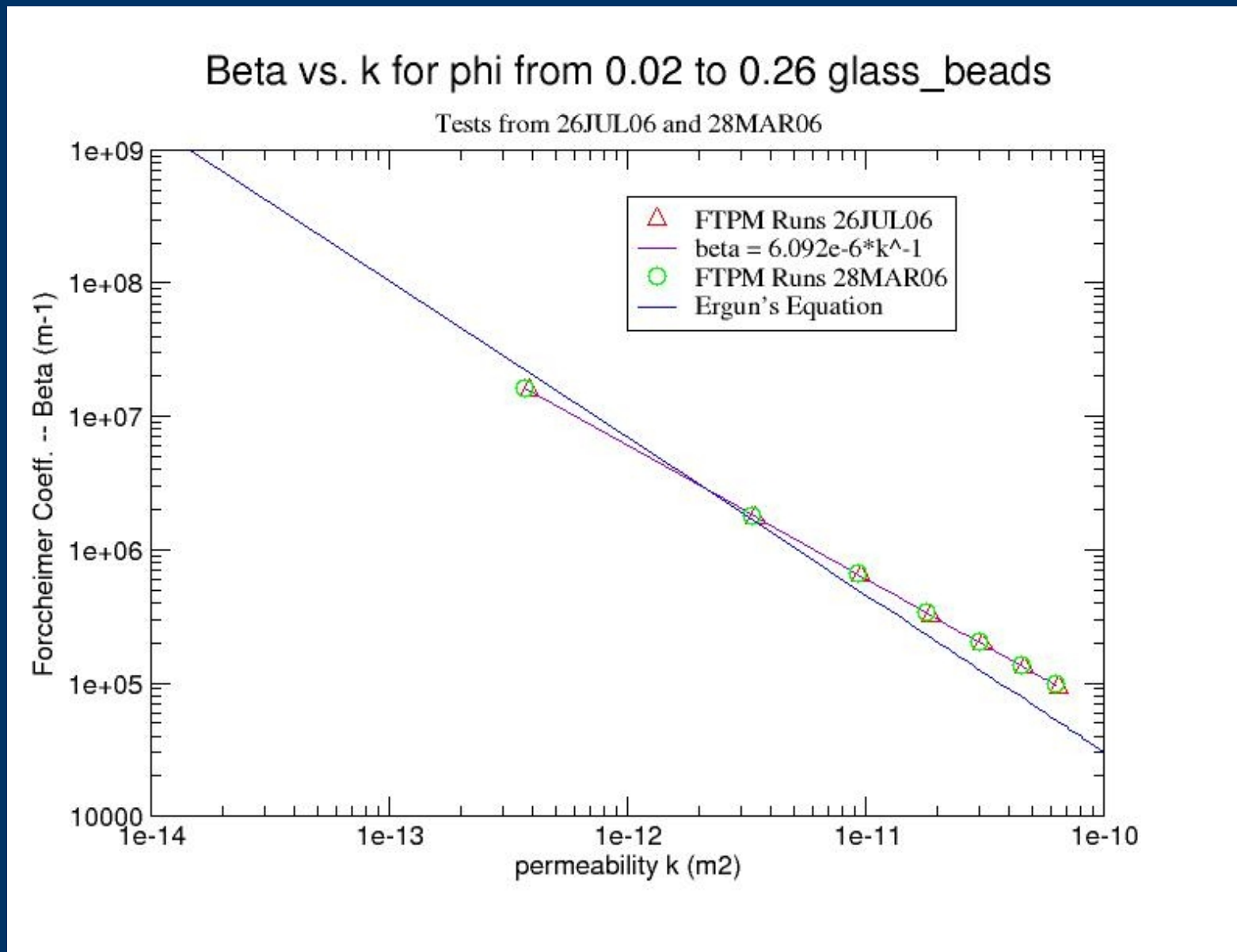
3D Monte Carlo networks from normal, beta, or empirical distribution (pore size pdf)

Coordination Number (1, 2, 3)

number of pores entering and leaving a junction
 $\theta \pm 90^\circ$

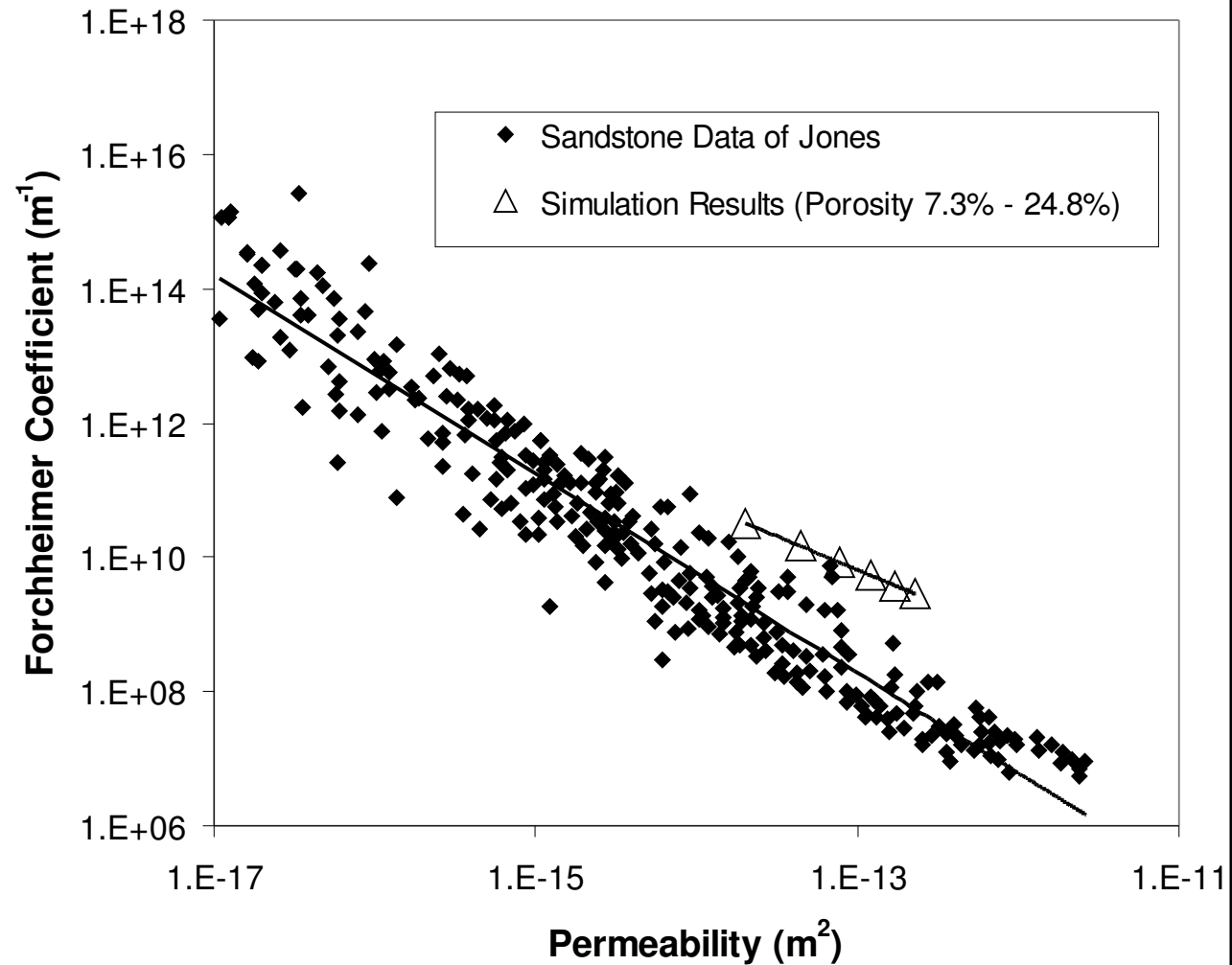


FTPm Results



FTPM Results

**Forchheimer Coefficient versus Permeability Comparison
of Simulation to Empirical Results**



Literature

T's and Y's – limited configurations and most are for turbulent flow

Basset, M.D., Winterbone, D.E., and Pearson, R.J., 2001, "Calculation of Steady Flow Pressure Loss Coefficients for Pipe Junctions," Proc. Instn. Mech. Engrs., Part C, Journal of Mechanical Engineering Science, **215** (8), pp. 861-881.

W.H. Hager, 1984, "An Approximate Treatment of Flow in Branches and Bends," Proc. Instn. Mech. Engrs., Part C, Journal of Mechanical Engineering Science, **198**(4) pp. 63-9.

Blaisdell, F.W., and Manson, P.W., 1967, "Energy loss at pipe junctions," J. Irrig. and Drainage Div., ASCE, **93**(IR3), pp. 59-78.

Schohl, G.A., 2003, "Modeling of Tees and Manifolds in Networks," *Proceedings of the 4th ASME/JSME Joint Fluids Engineering Conference*, **2**, Part D, pp. 2779-2786.

Bassett, M.D., Pearson, R.J., and Winterbone, D.E., 1998, "Estimation of Steady Flow Loss Coefficients for Pulse Converter Junctions in Exhaust Manifolds," *IMEchE Sixth International Conference on Turbocharging and Air Management Systems*, IMechE HQ, London, UK, **C554/002**, pp.209-218.

Ruus, E., 1970, "Head Losses in Wyes and Manifolds," J. Hyd. Div., ASCE, **96**(HY3), 593-608.

Laminar loss coefficients and elbows, reductions, contractions – much *larger loss coefficients than turbulent case – strong dependence on Reynold's number.*

Edwards, M.F., Jadallah, M.S.M., and Smith, R., 1985, "Head Losses in Pipe Fittings at Low Reynolds Numbers," Chem. Engr. Res. Des., **63**(1), pp. 43-50.

Importance of roughness at microscale

The slide concludes with a series of four horizontal bars of varying lengths and colors (orange, grey, orange, grey) extending from the left edge.

Problem Description

Stagnation Loss Coefficient

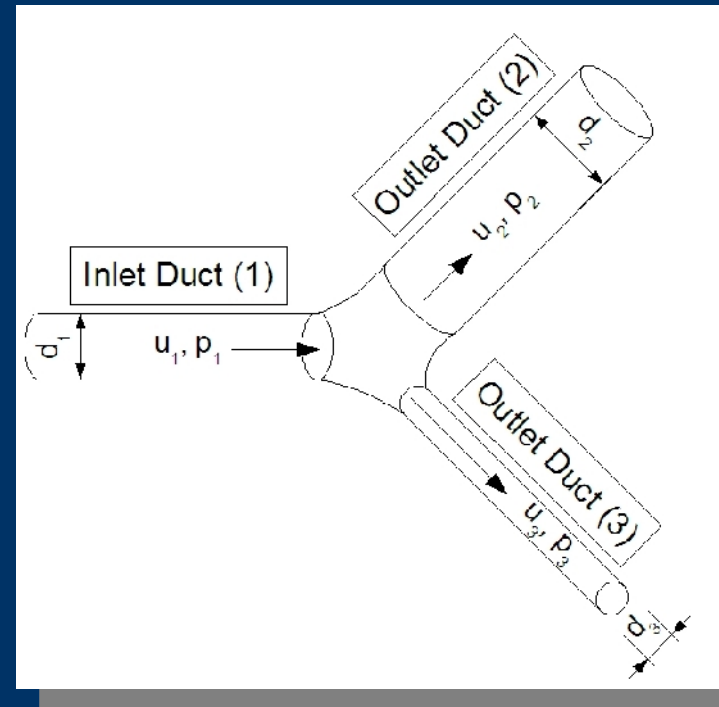
$$K_2 = \frac{\left[\left(\frac{p_1}{\rho} + \frac{u_1^2}{2} \right) - \left(\frac{p_2}{\rho} + \frac{u_2^2}{2} \right) \right]}{\frac{u_1^2}{2}}$$

Parameters:

d_2/d_1 , d_3/d_1

θ_2 and θ_3

f_2 (this sets f_3) – (why? other literature and possibility of simulations where this is unknown initially)



Automation of Geometry Generation and CFD Runs

Custom Code was written to:

- (a) create GAMBIT journal files that instantiate the desired geometry based on existing 2D geometries.
- (c) create a script that loads journal files into GAMBIT and meshes
- (d) create all necessary preprocessing files for FLUENT.
- (e) create post-processing files for FLUENT results and to tabulate results for a complete set of runs

Solution Methodology

2D Geometry Generalization

$$L_1 = 5 d_{\max}$$

$$L_2 \text{ and } L_3 = 10 d_{\max}$$

If $d_2 > d_{\text{avg}}$,
then $r_2 = 3d_2$;

else $r_2 = 2d_2$

If $d_3 > d_{\text{avg}}$,
then $r_3 = 3d_3$;

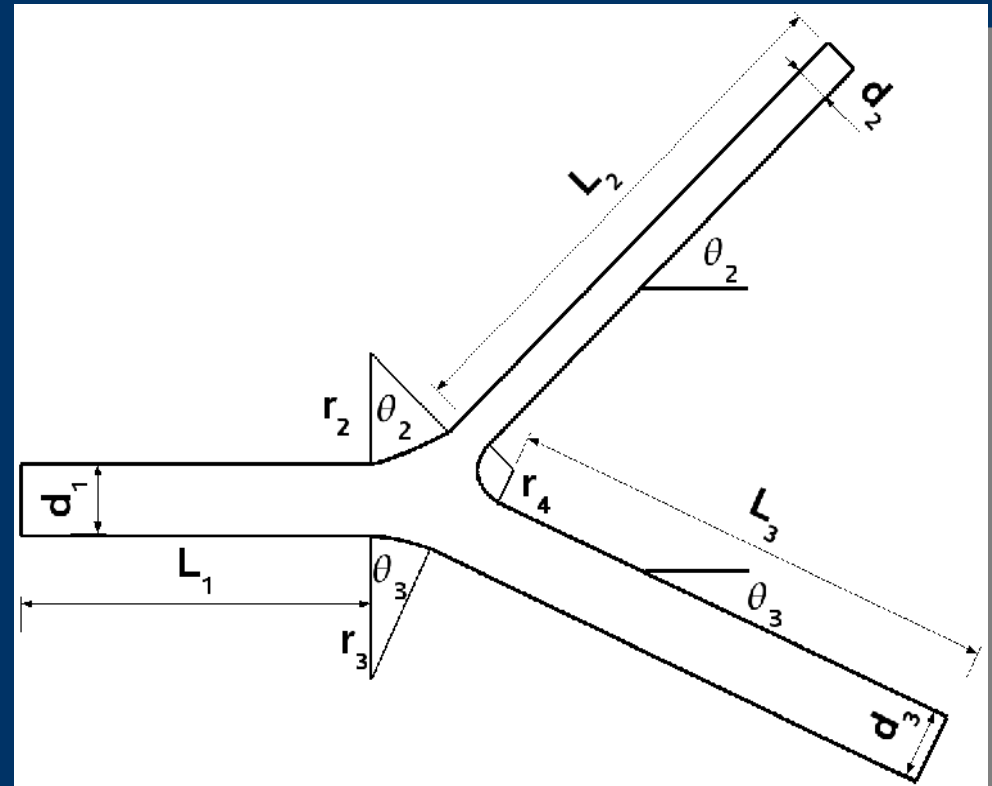
else $r_3 = 2d_3$

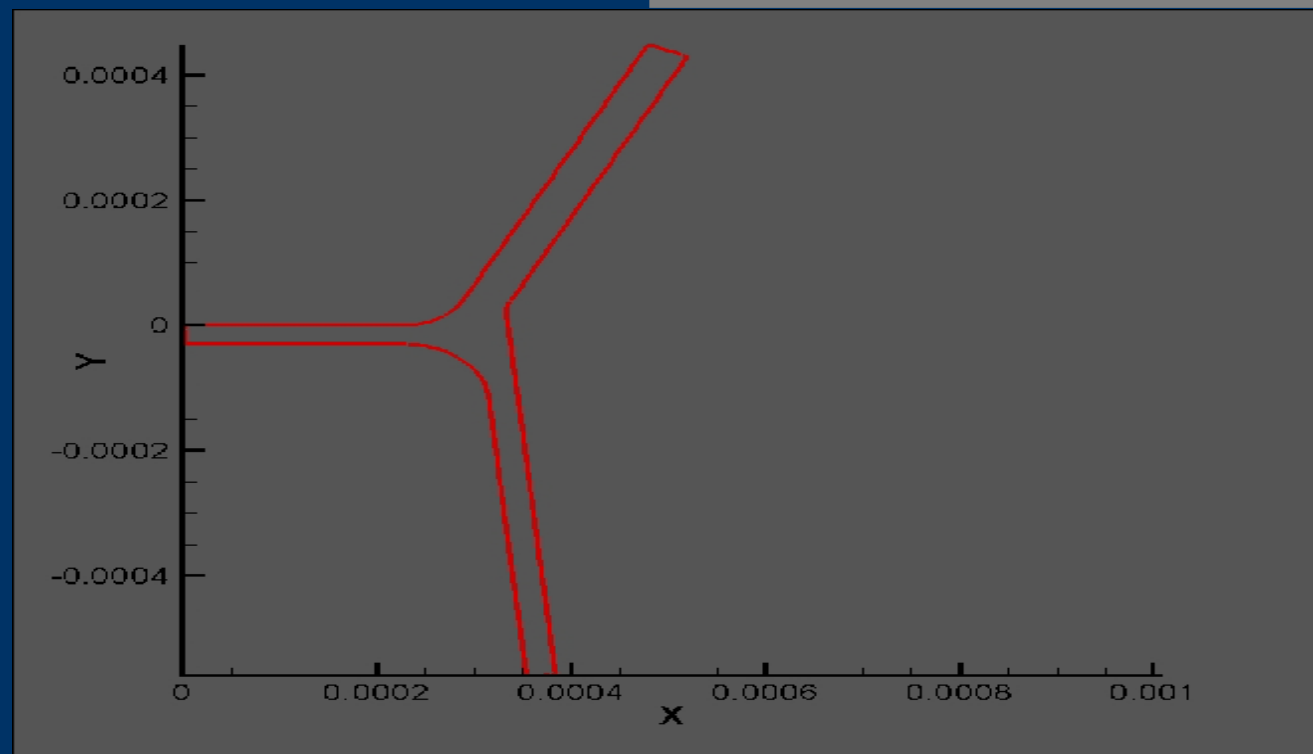
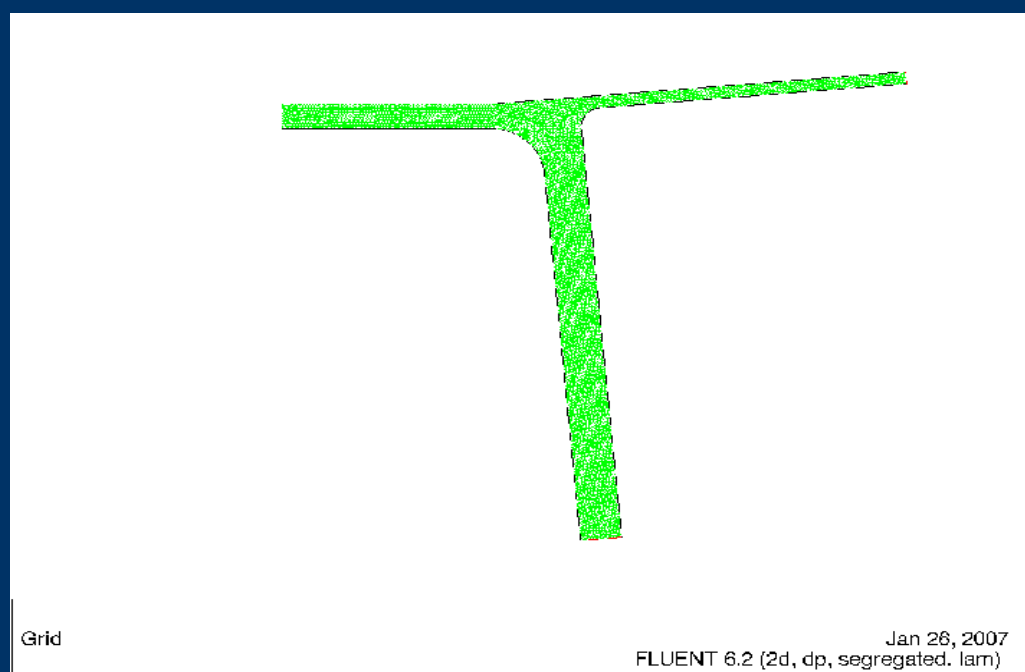
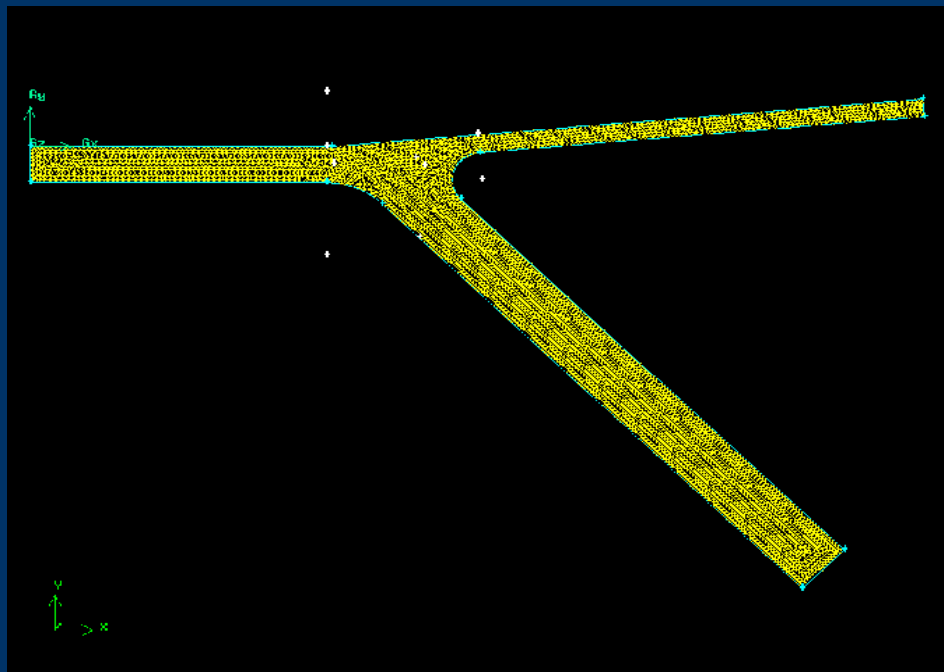
$$r_4 = d_{\max} / 2$$

Generalized Geometry

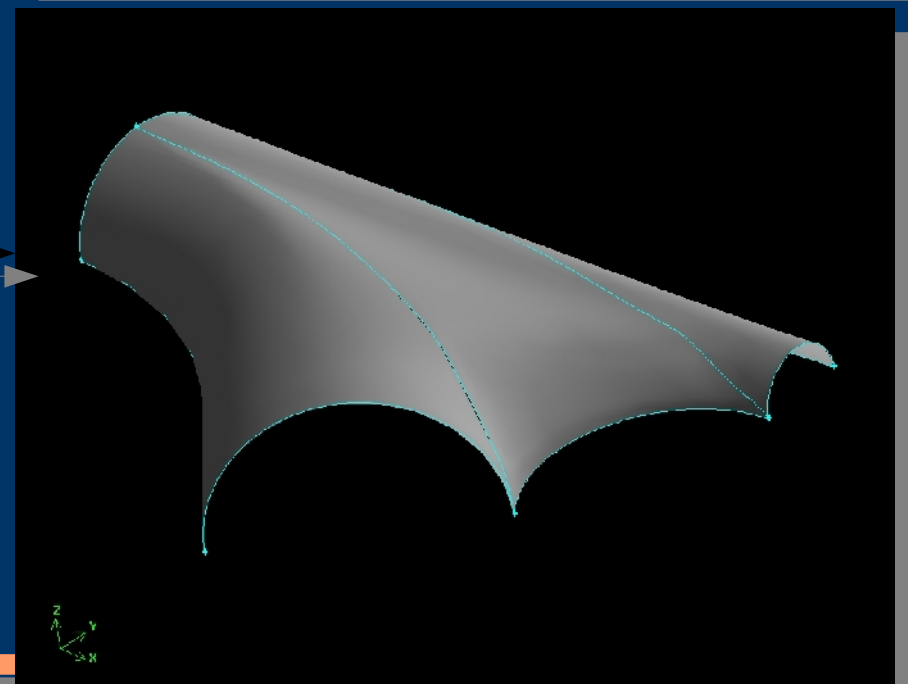
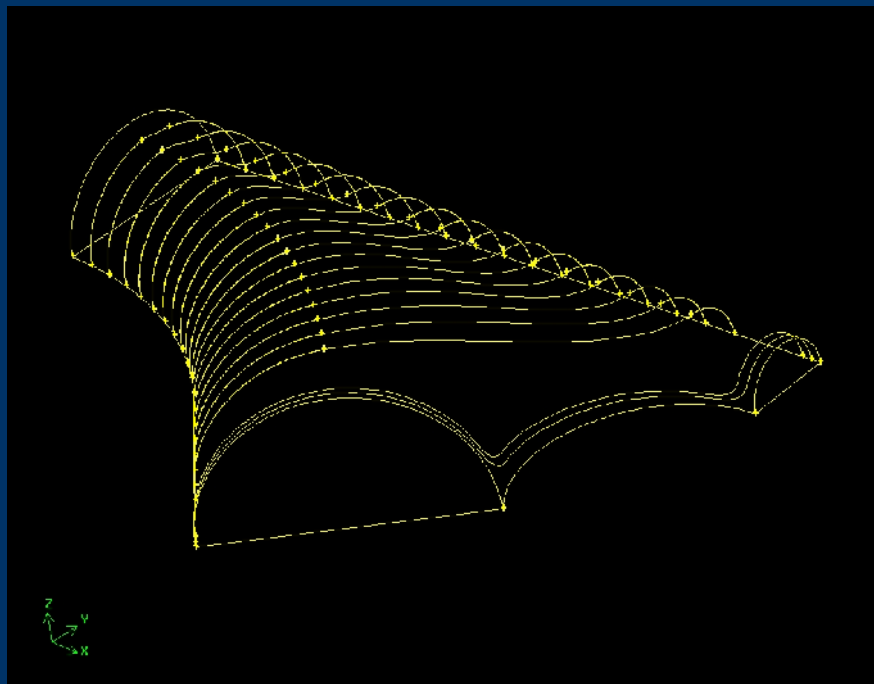
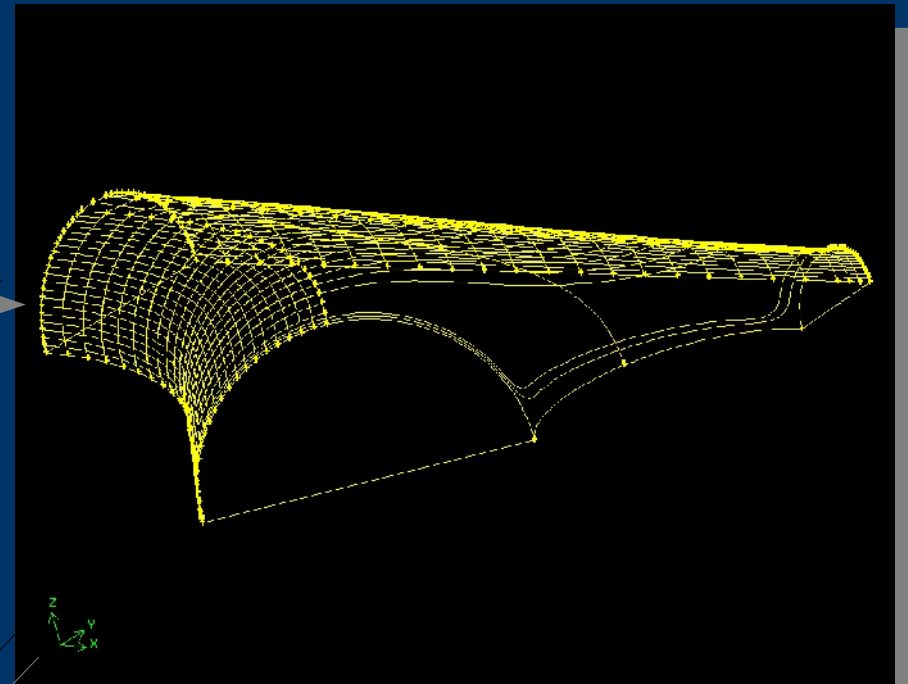
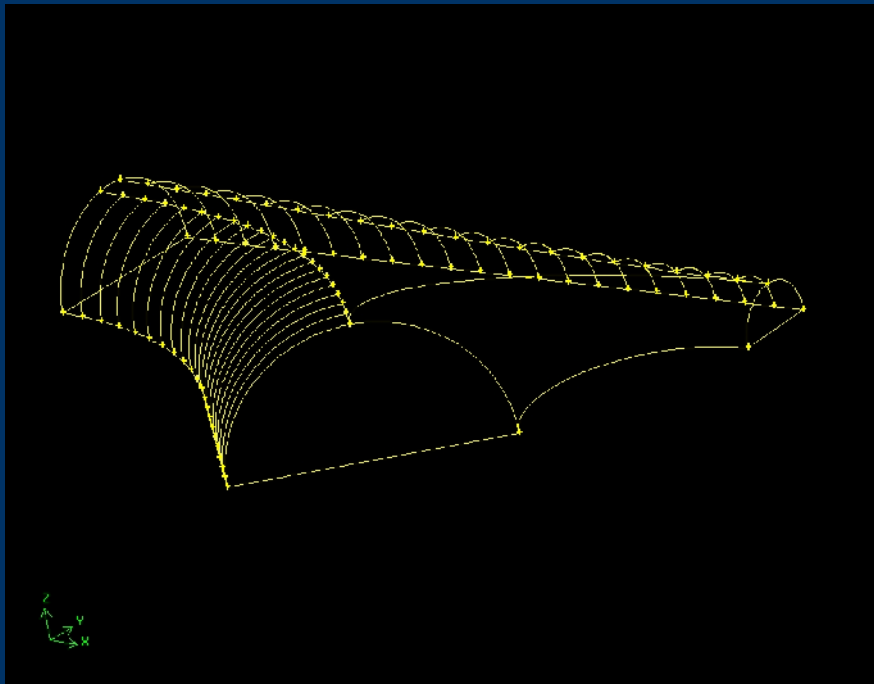
larger and smaller outlet ducts ; 2Dim. - 3Dim are underway

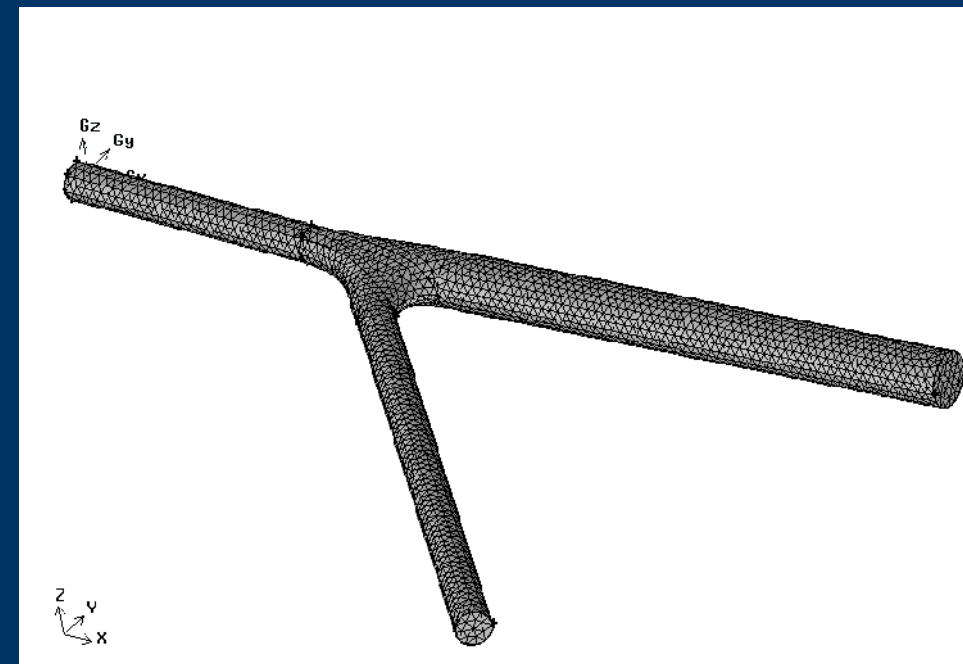
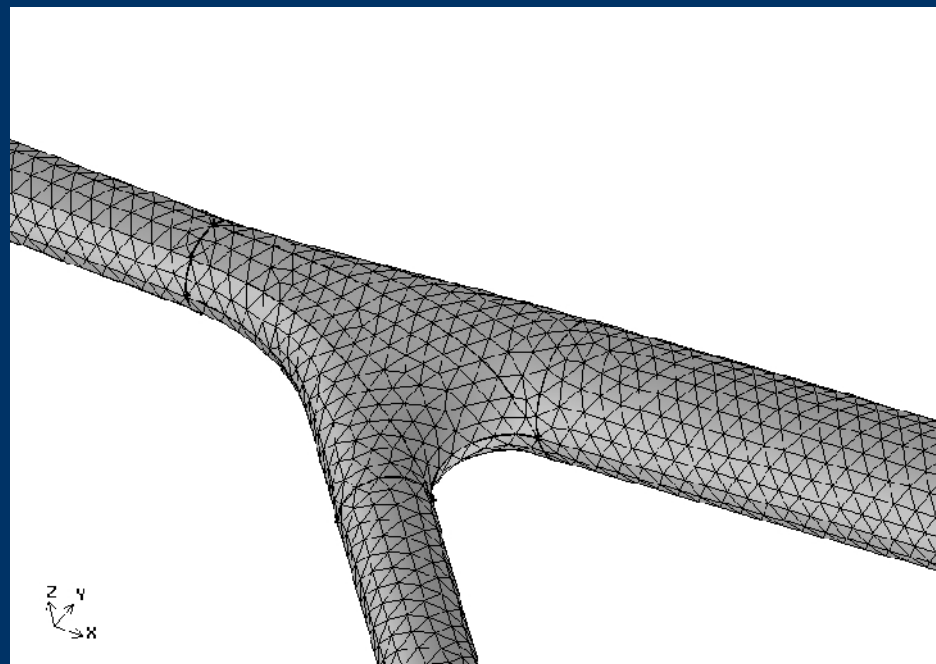
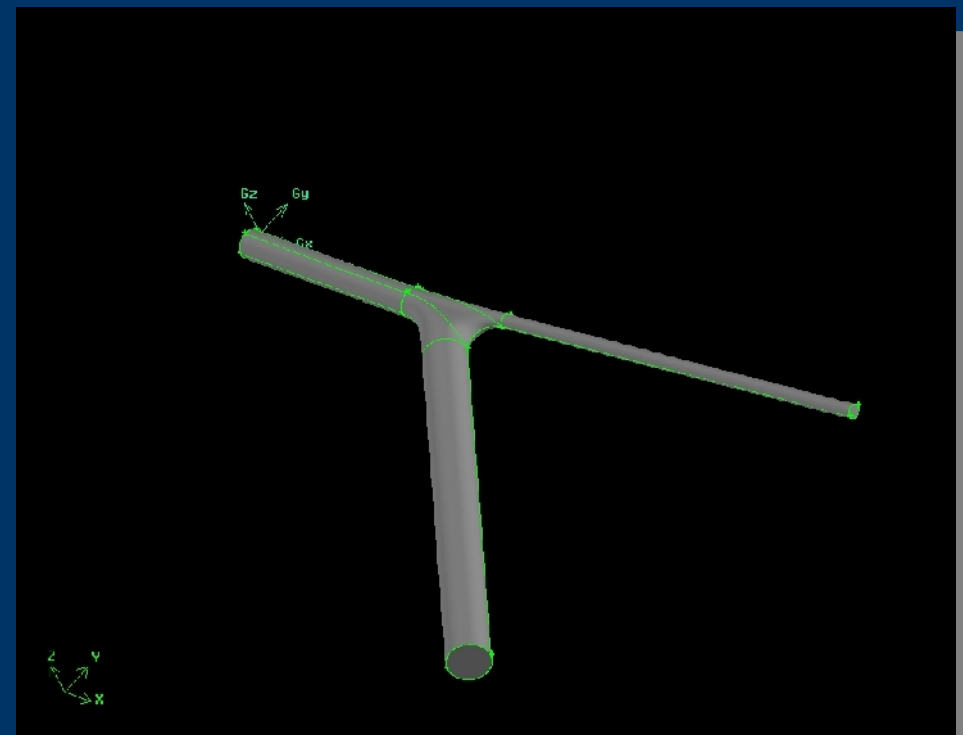
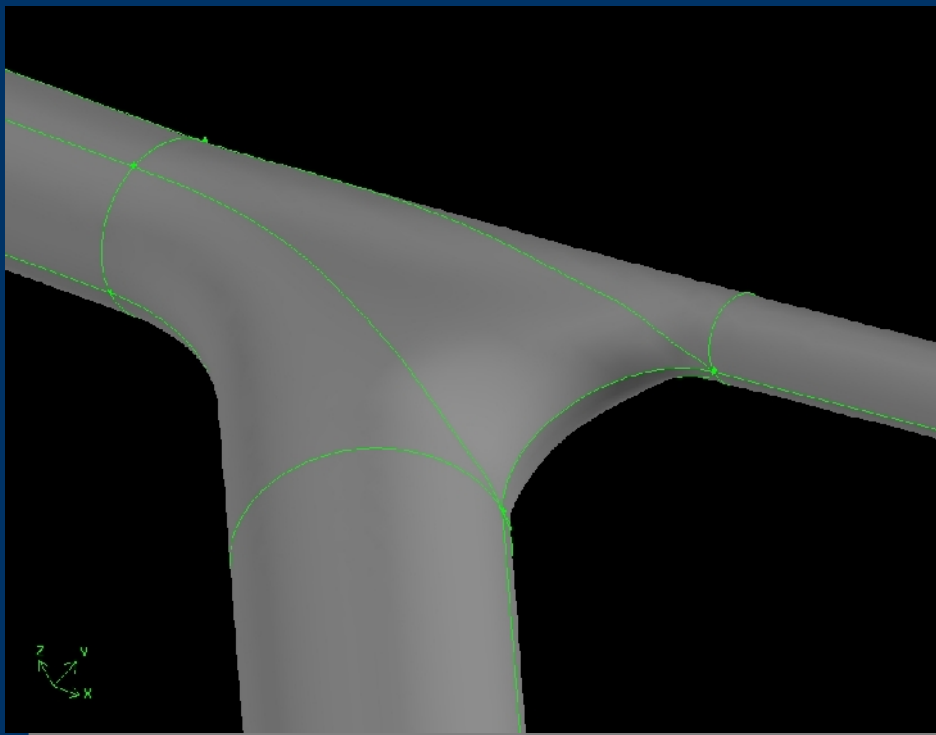
avoid sharp edges ; 5 – 90 degrees for angles





3D Geometry – Mark I





Simulation Parameters

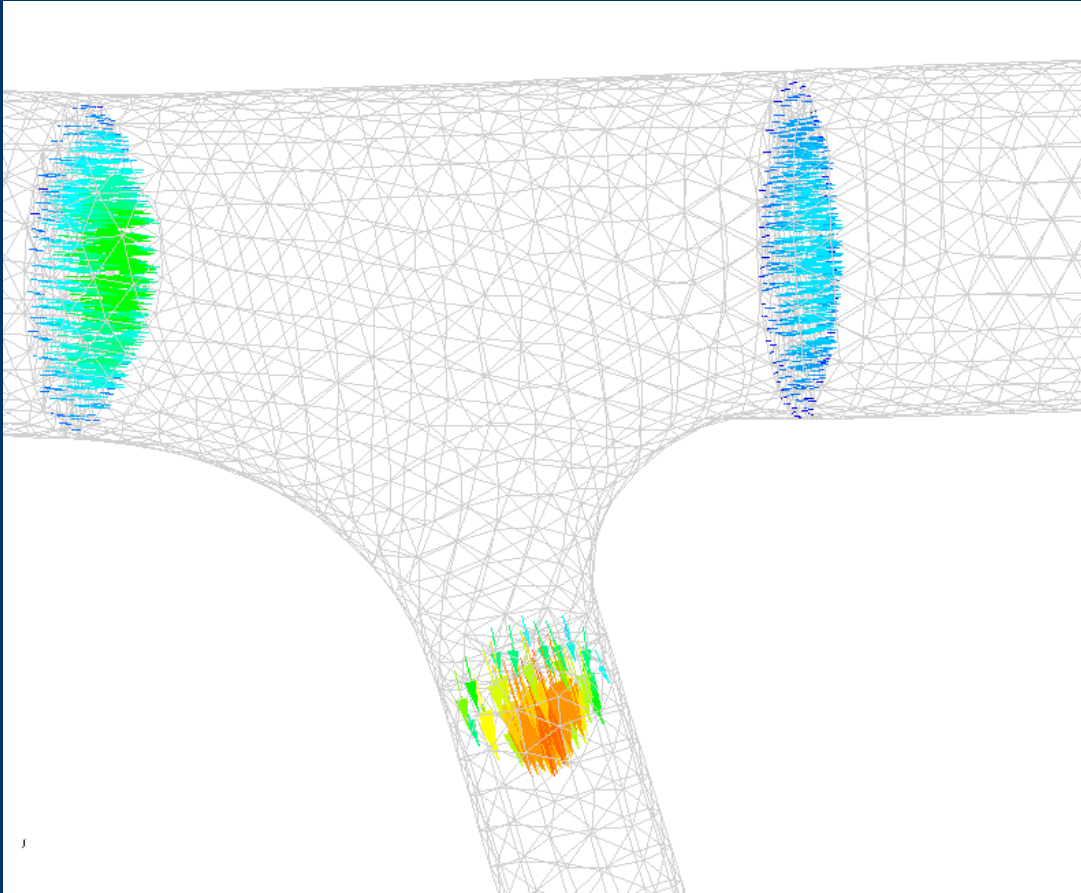
Re_D was maintained at constant value at the inlet duct

d_1 was 30 microns. The fluid was chosen to be liquid water at 20°C. The inlet flow velocity, u_1 , was set to 0.5 m/s giving a Reynolds number of 15

$Le_D = 0.06 Re_D D$ --- gives 0.9 D for $Re_D = 15$

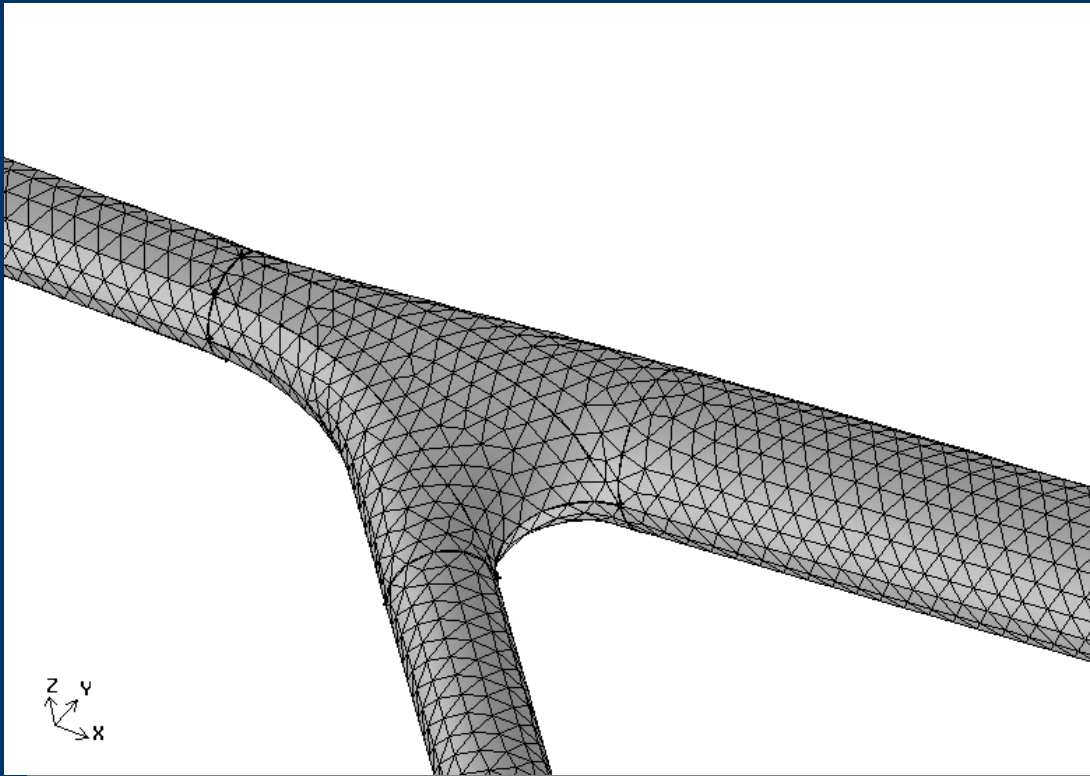
FLUENT output files contain surface averaged static pressure and magnitude of flow velocity at duct cross-sections at the duct inlets and exits.

Duct Inlet/Outlets



Duct inlet and exit sections considered to be where geometry of duct is the same as the downstream portion for outlets and upstream portion for inlet.

Mesh Automation



Mesh was set to 1/4 of smallest duct

Tetrahedral Mesh

Large number of tests to assess ability to generalize the mesh (1/4 factor determined in this manner)

Some testing to verify no change in results with change in mesh size.

Inlet was specified as velocity inlet

Outlets were outflow boundaries – allowed specification of flow fraction

Numerical Methods

Finite Volume solution of integral Navier Stokes

Steady-State 3D

Implicit

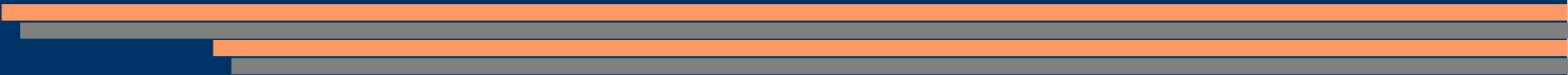
SIMPLE for pressure velocity coupling

1st order upwind scheme of momentum

discretization

Max number of iterations

Convergence criterion = 0.1%



Parameter Values

d_2/d_1 and $d_3/d_1 = 0.5, 1.0, 1.5$

$f_2 = 0.1, 0.3, 0.5, 0.7, 0.9$

θ_2 and $\theta_3 = 5^\circ, 25^\circ, 45^\circ, 65^\circ, 85^\circ$

600 runs attempted – 475 completed (*geometry issues on remainder*)

Suite of C++ procedures to create geometries, input files, read and collate results

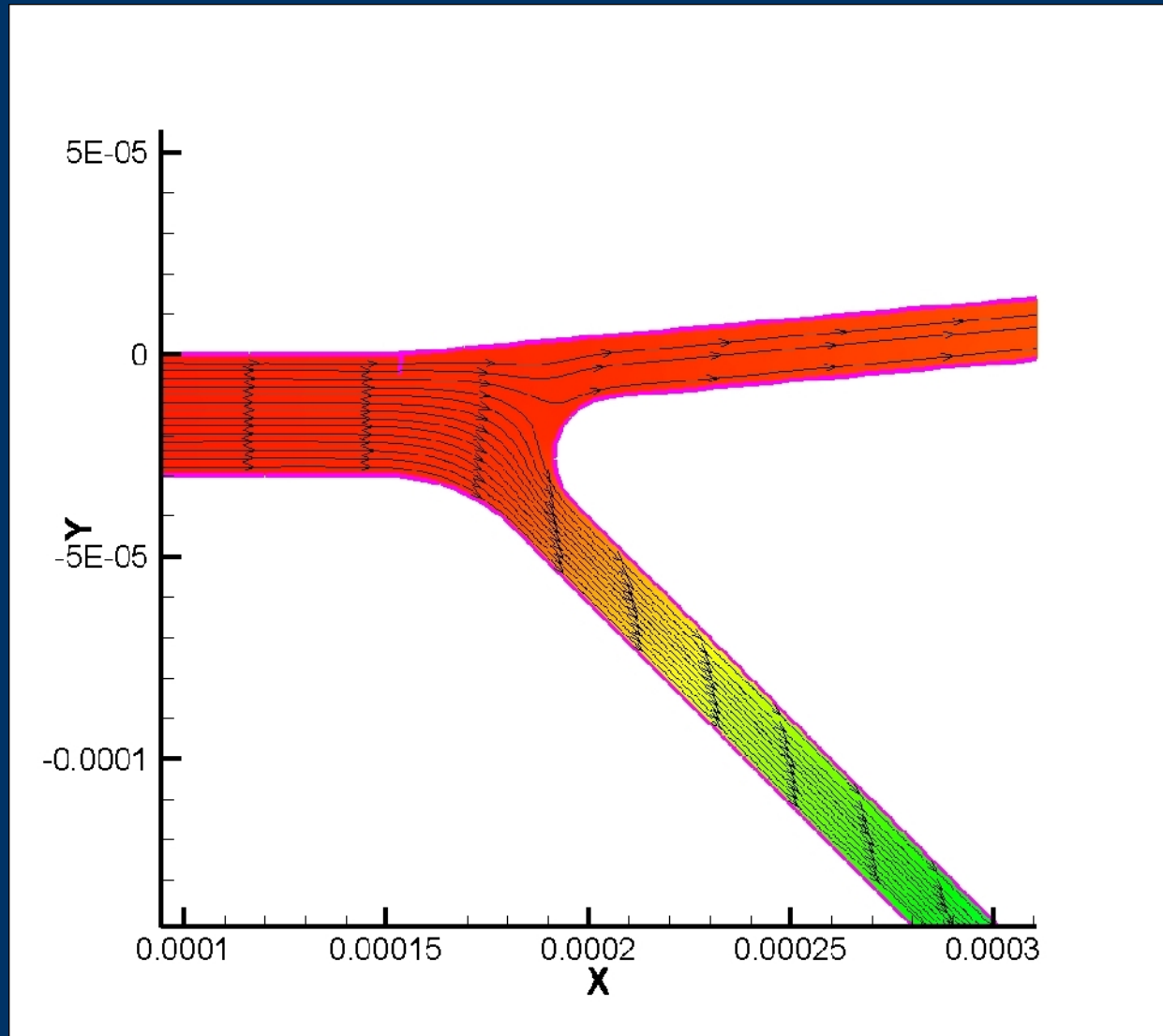
Create GAMBIT script to create geometries

Create input files for GAMBIT and FLUENT

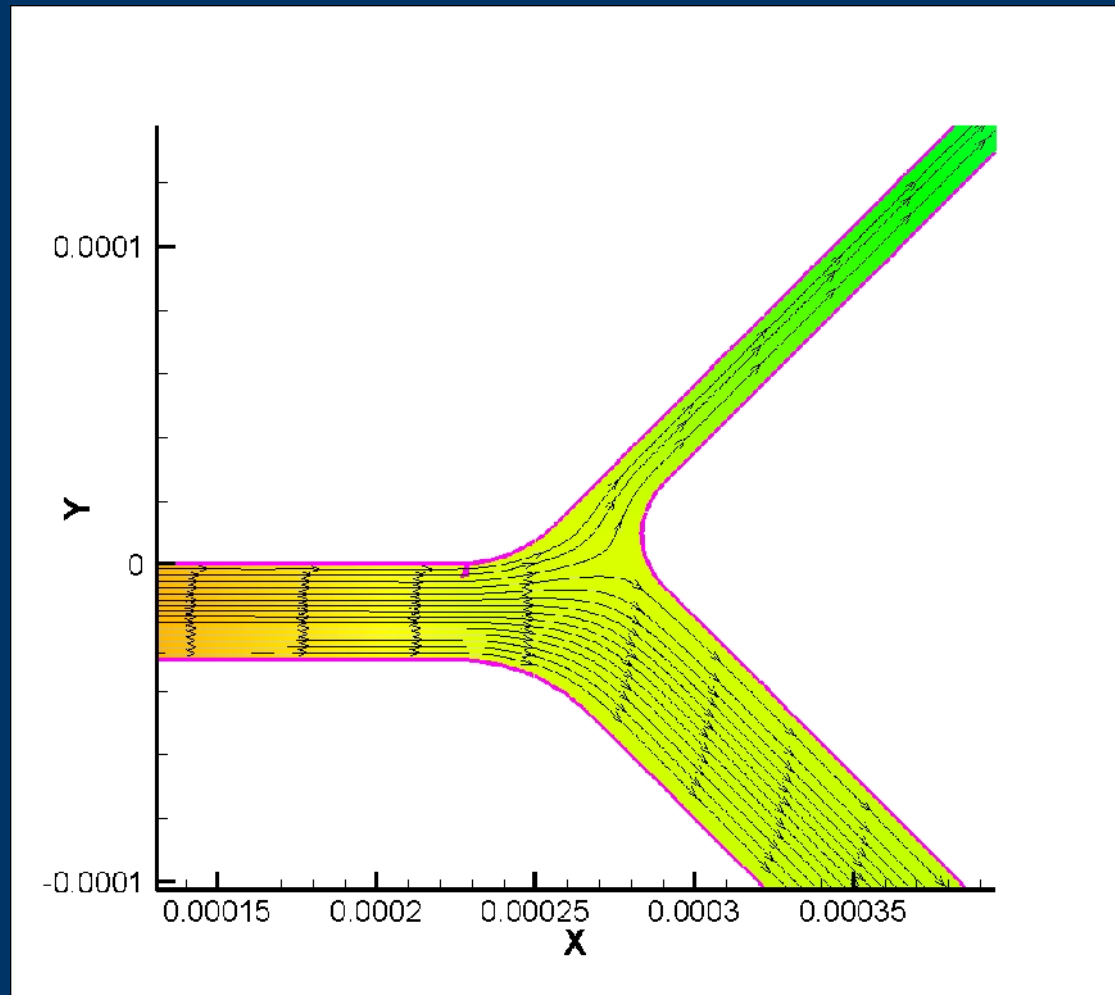
Read results files for static pressures and velocities averaged over surfaces in and out of junctions.

Fluent Result

$f_2 = 0.1$, $d_2/d_1 = 0.5$, $\theta_2 = 5^\circ$, $d_3/d_1 = 0.5$, and $\theta_3 = 45^\circ$

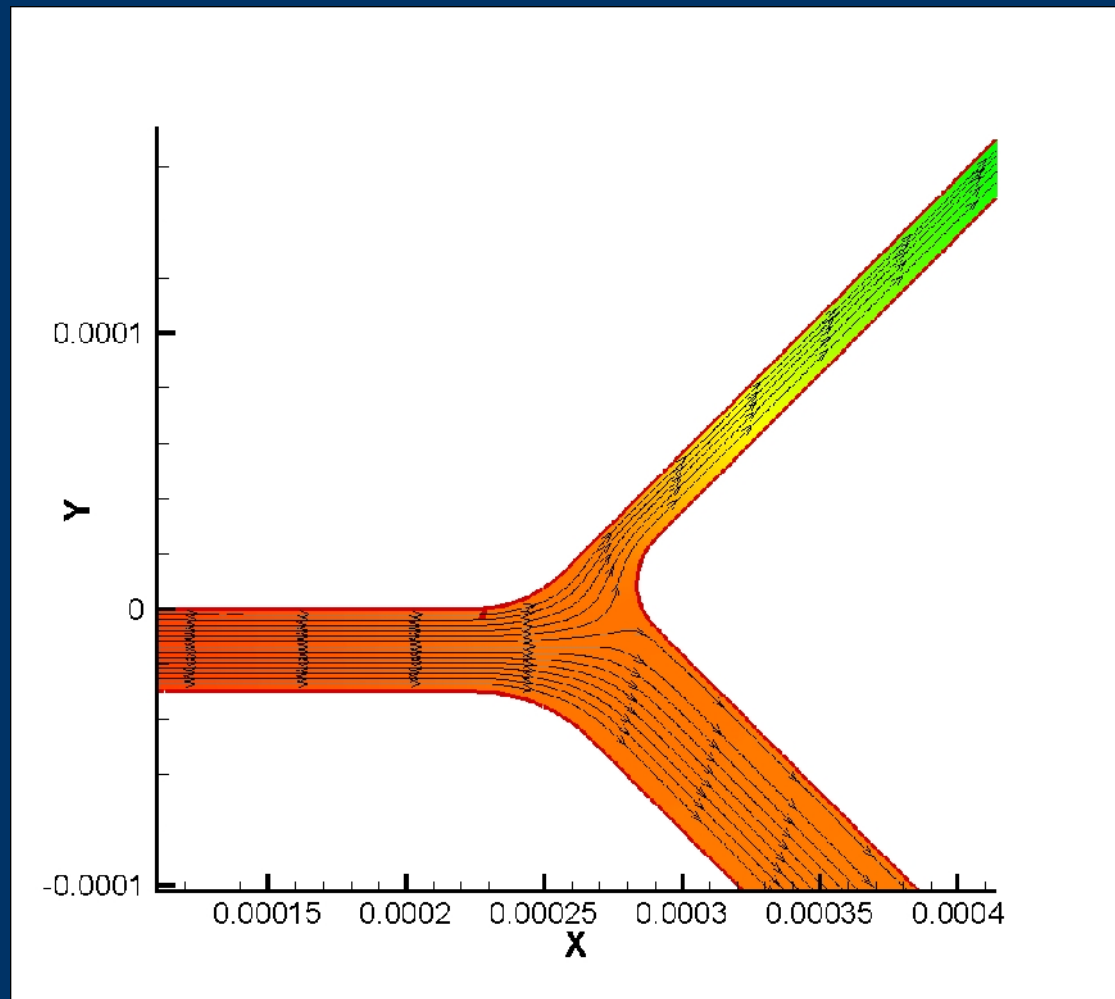


$f_2 = 0.1$, $\theta_2 = 45^\circ$, $\theta_3 = 45^\circ$, $d_2/d_1 = 0.5$, $d_3/d_1 = 1.5$.



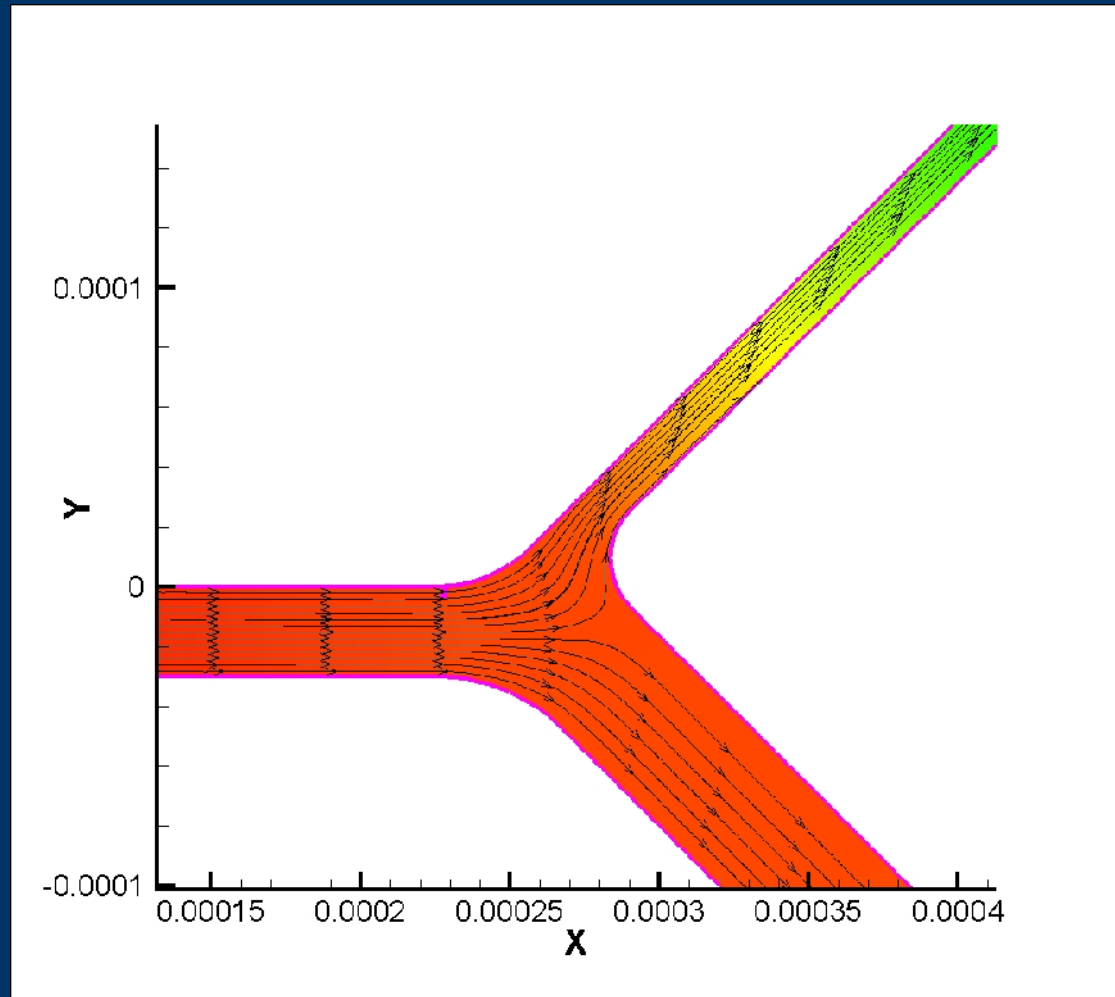
$$K_2 = 5.47$$

$f_2 = 0.3$, $\theta_2 = 65^\circ$, $\theta_3 = 45^\circ$, $d_2/d_1 = 0.5$, $d_3/d_1 = 1.5$.



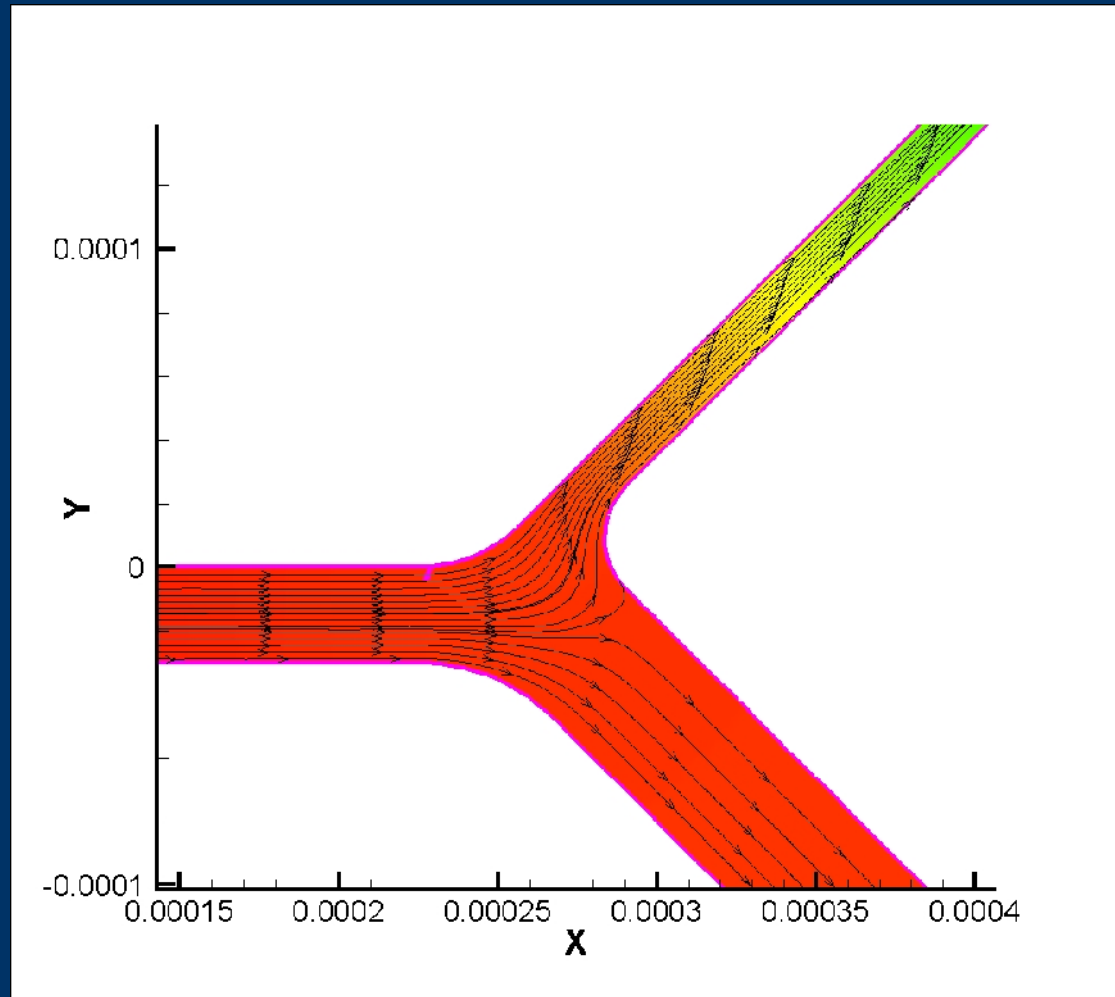
$$K_2 = 11.6$$

$f_2 = 0.5$, $\theta_2 = 65^\circ$, $\theta_3 = 45^\circ$, $d_2/d_1 = 0.5$, $d_3/d_1 = 1.5$.



$$K_2 = 18.4$$

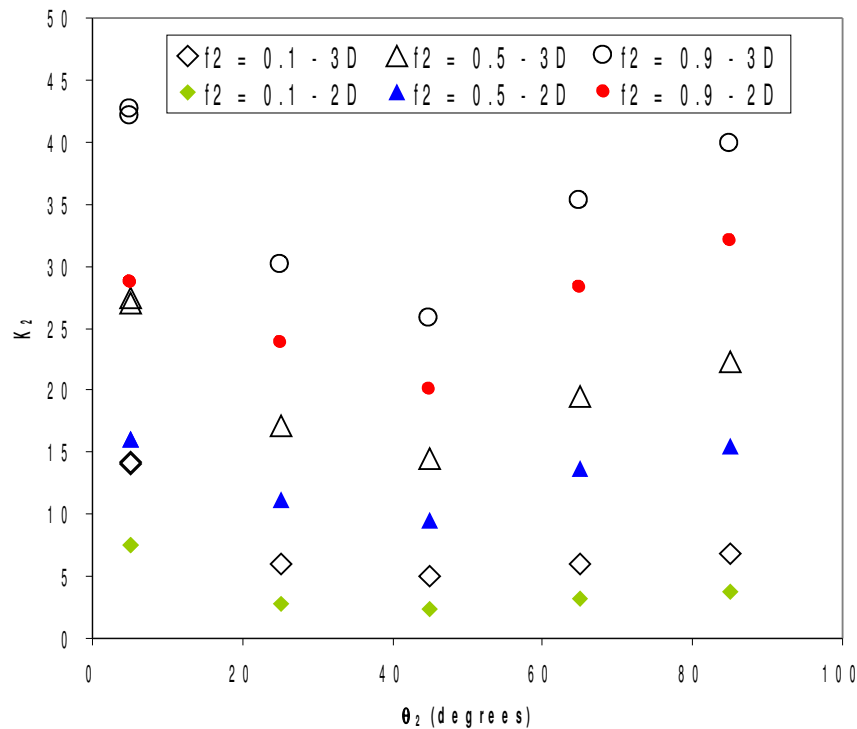
$f_2 = 0.7$, $\theta_2 = 65^\circ$, $\theta_3 = 45^\circ$, $d_2/d_1 = 0.5$, $d_3/d_1 = 1.5$.



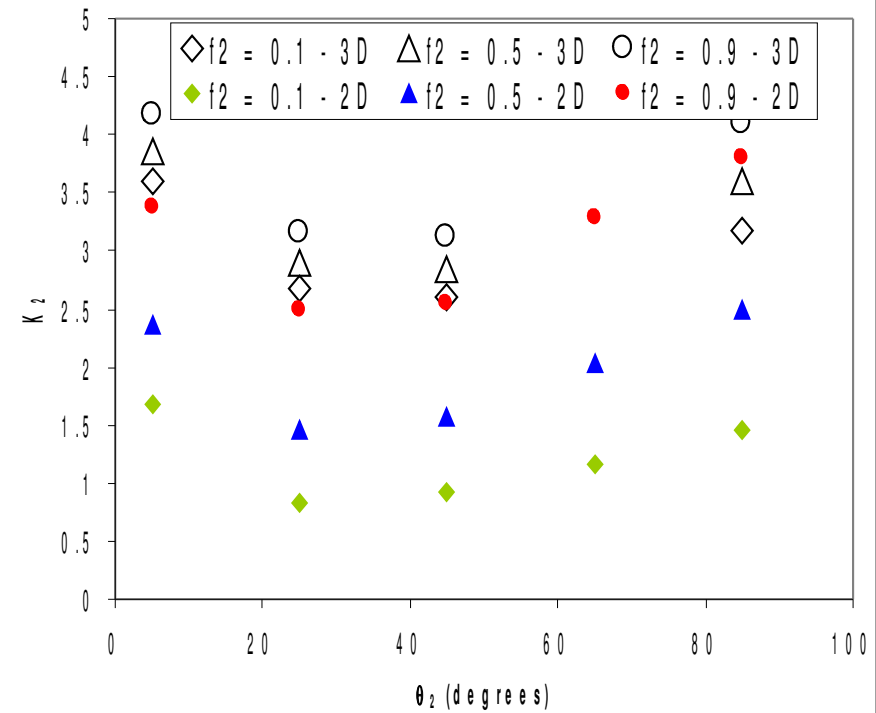
$$K_2 = 25.7$$

2D vs. 3D Differences

K_2 values for $d_2/d_1 = 0.5$, $d_3/d_1 = 0.5$, $\theta_3 = 5$ degrees



K_2 values for $d_2/d_1 = 0.5$, $d_3/d_1 = 1.5$, $\theta_3 = 45$ degrees

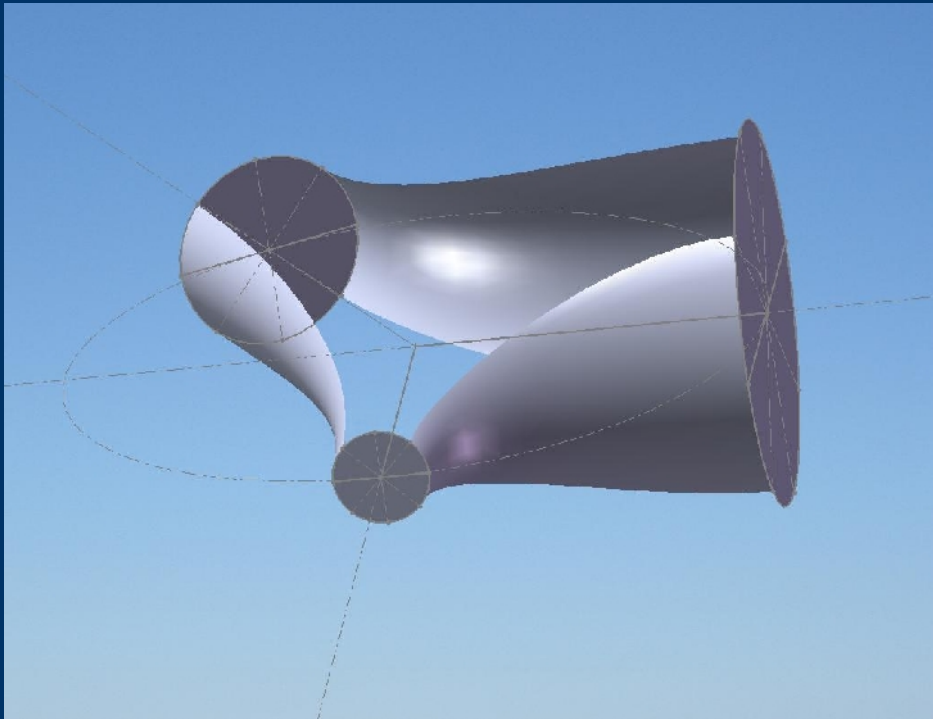


$$\left[\frac{k_2^{3D}}{k_2^{2D}} \right]_{average} = 1.55 \quad (std. \ dev.) = 0.45$$

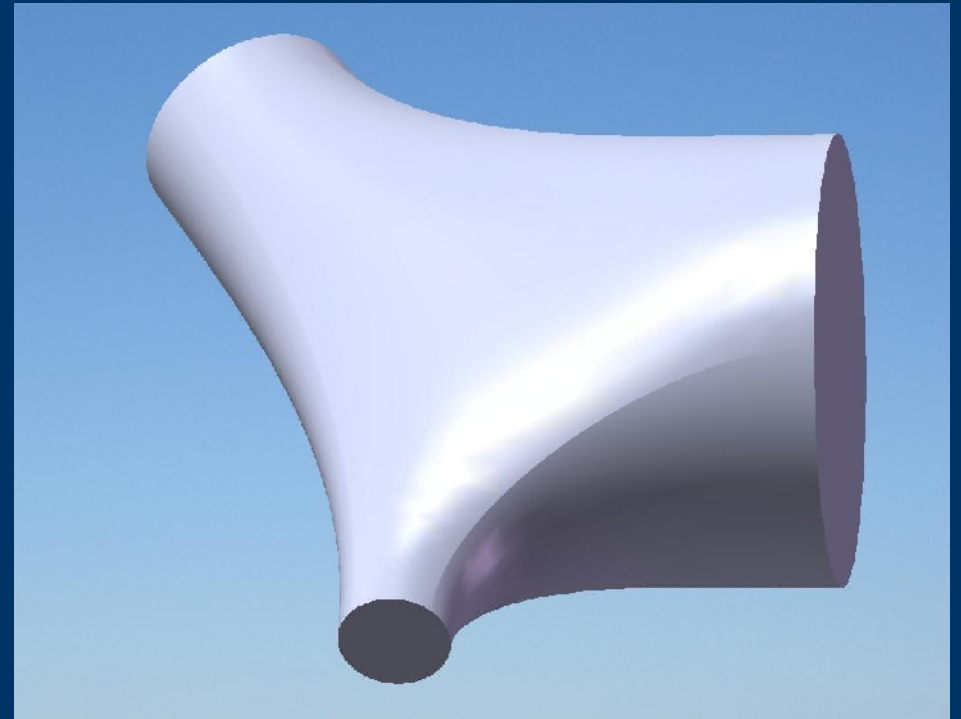
$$k_2 = \frac{\Delta p / \rho}{u_1^2 / 2} - \frac{u_2^2}{u_1^2} + 1$$

pressure effects kinetic energy effects

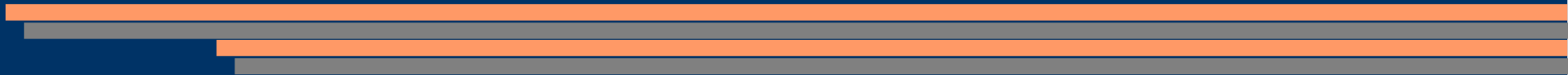
3D Mark II Junction



Junction Without Surface Fills



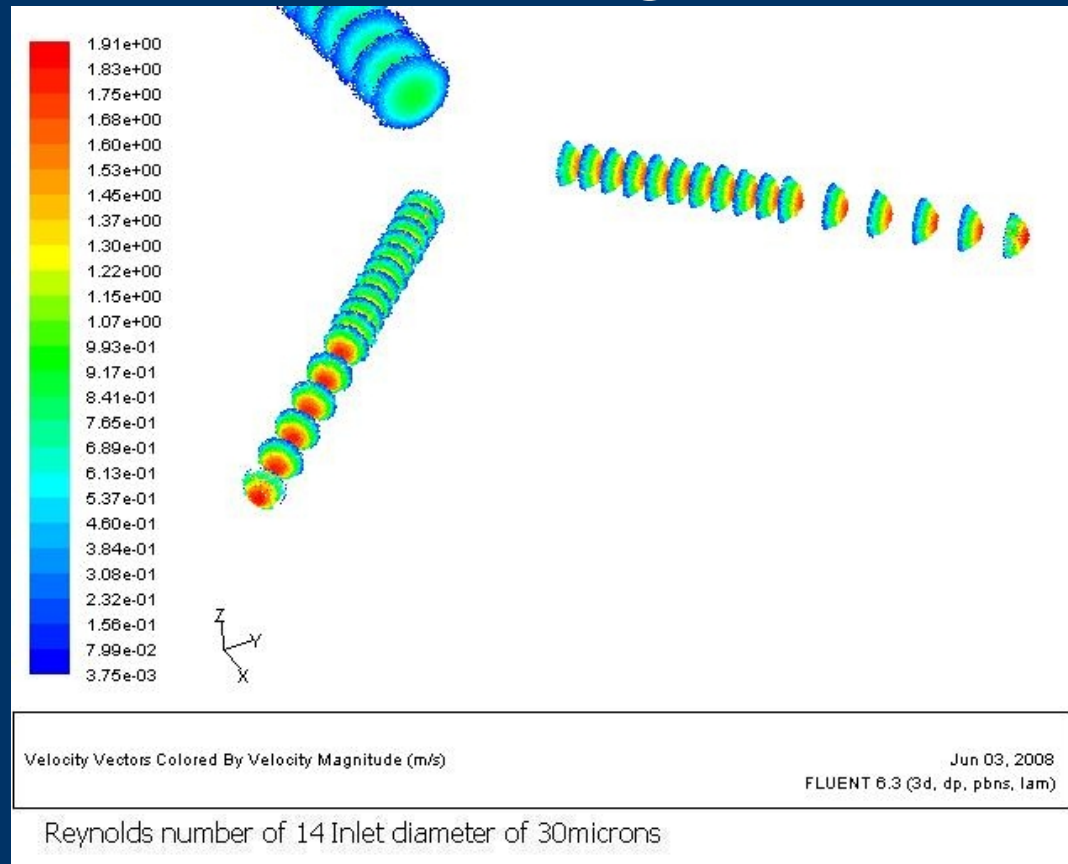
Junction With Surface Fills

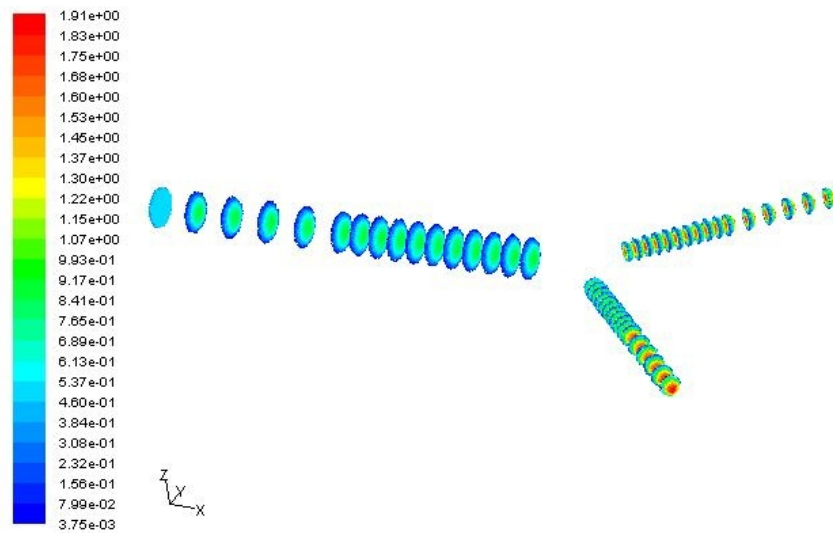


Initial Simulations – 3D Mark II

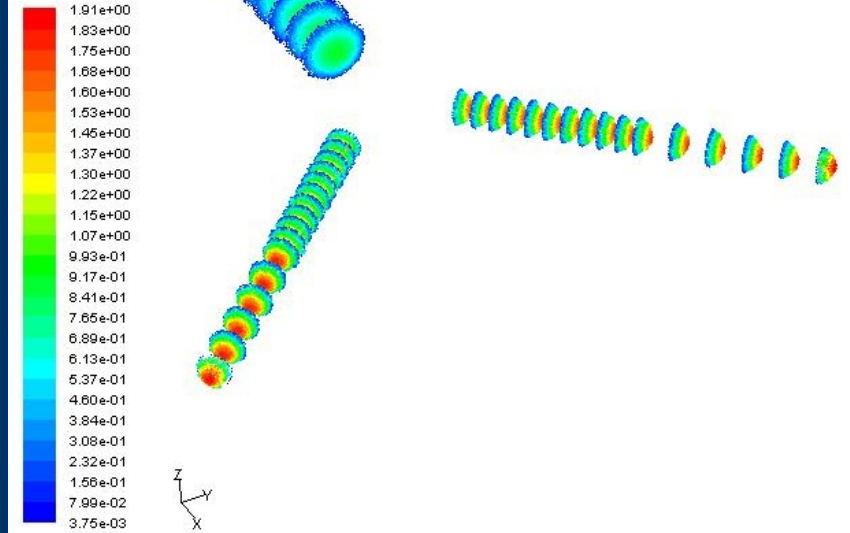
Small batch

Comparable results to original 3D runs

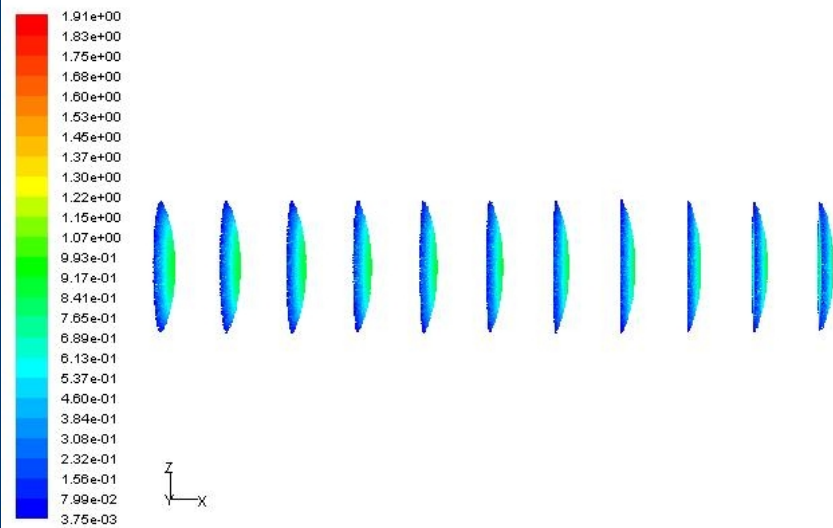




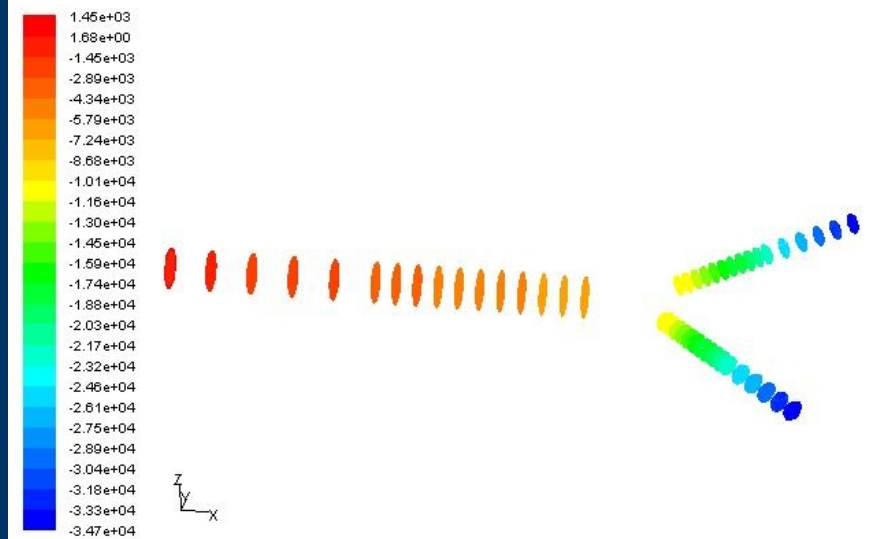
Reynolds number of 14 Inlet diameter of 30microns



Reynolds number of 14 Inlet diameter of 30microns



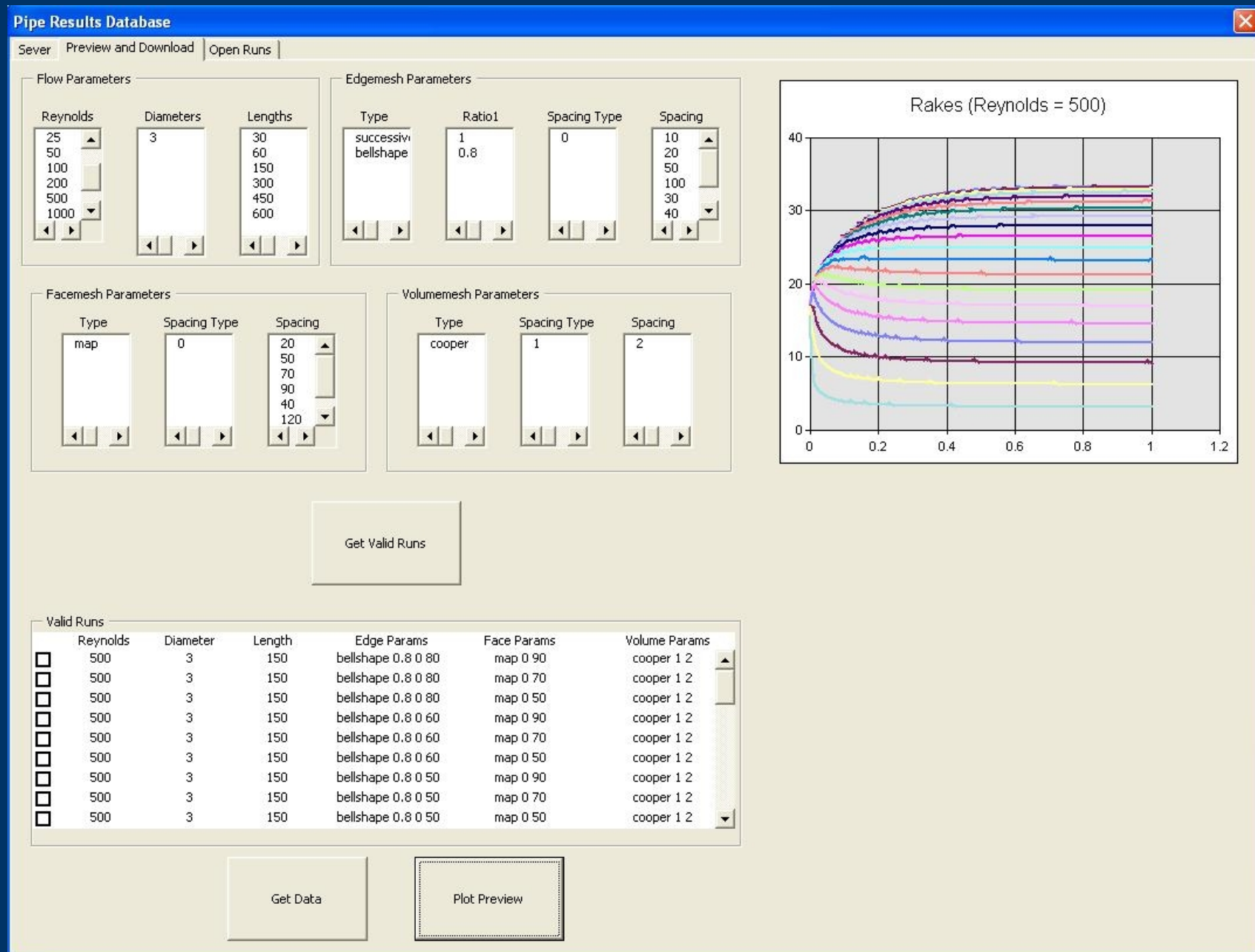
Reynolds number of 14 Inlet diameter of 30microns



Reynolds number of 14 Inlet diameter of 30microns

Pipe Mesh Testing

Database Interface



Pipe Mesh Testing

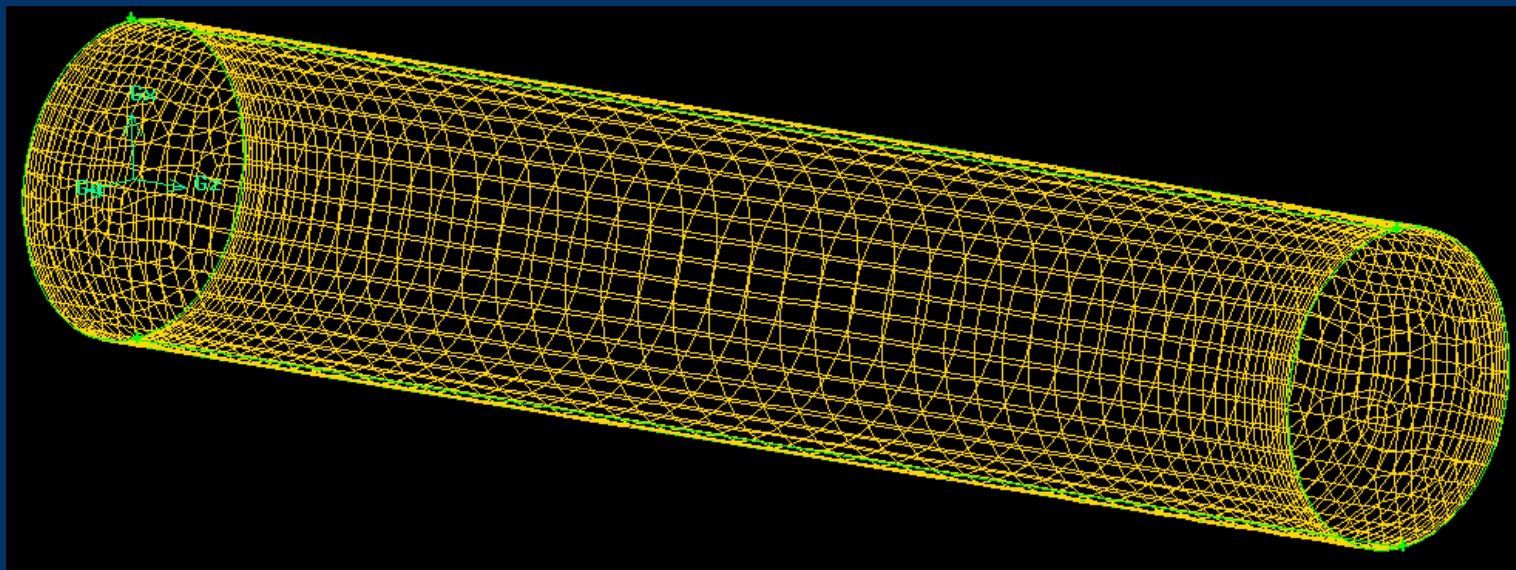
Flow-aligned hex core

Varied axial and radial spacing

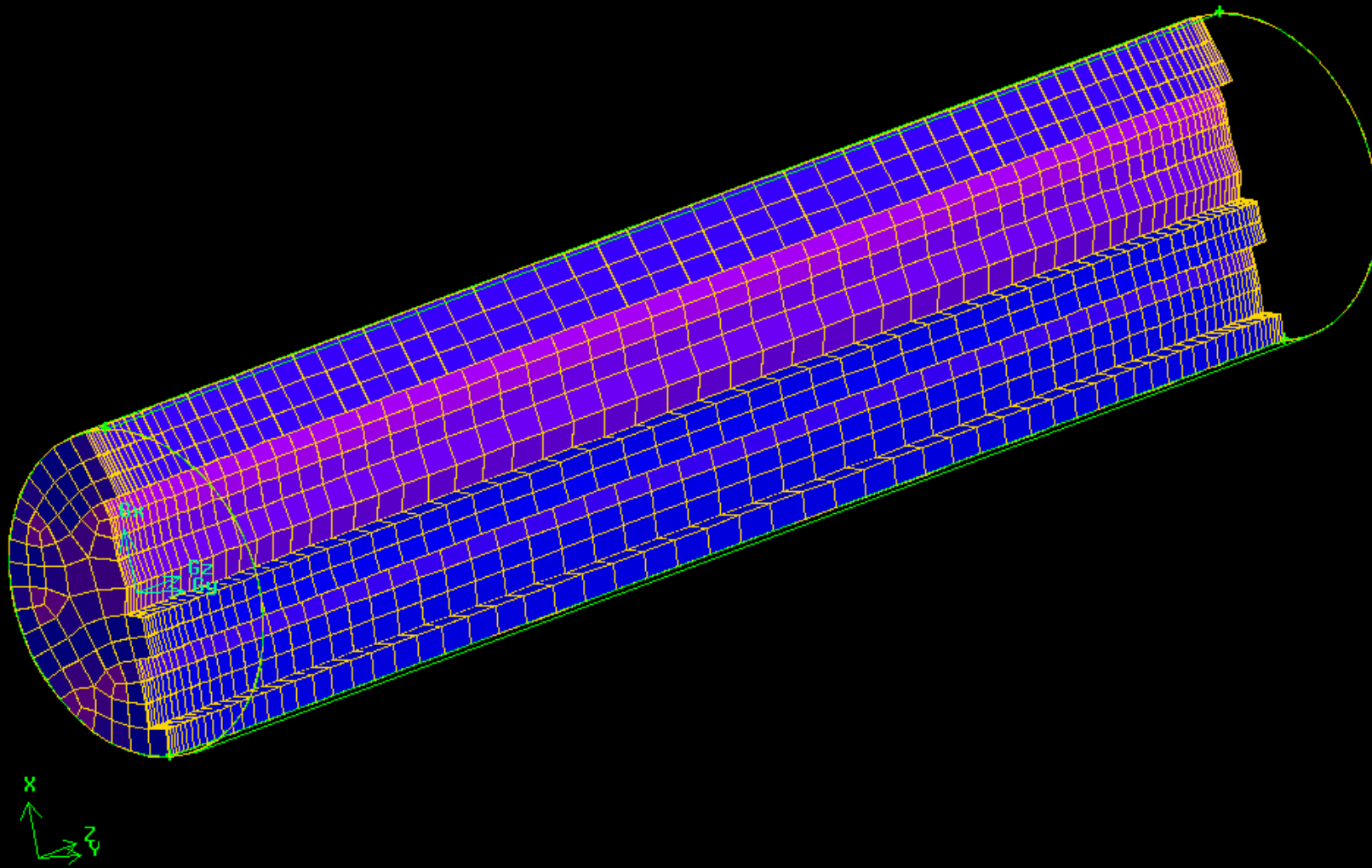
MySQL results database

Automated

Results database easy to setup for junction runs

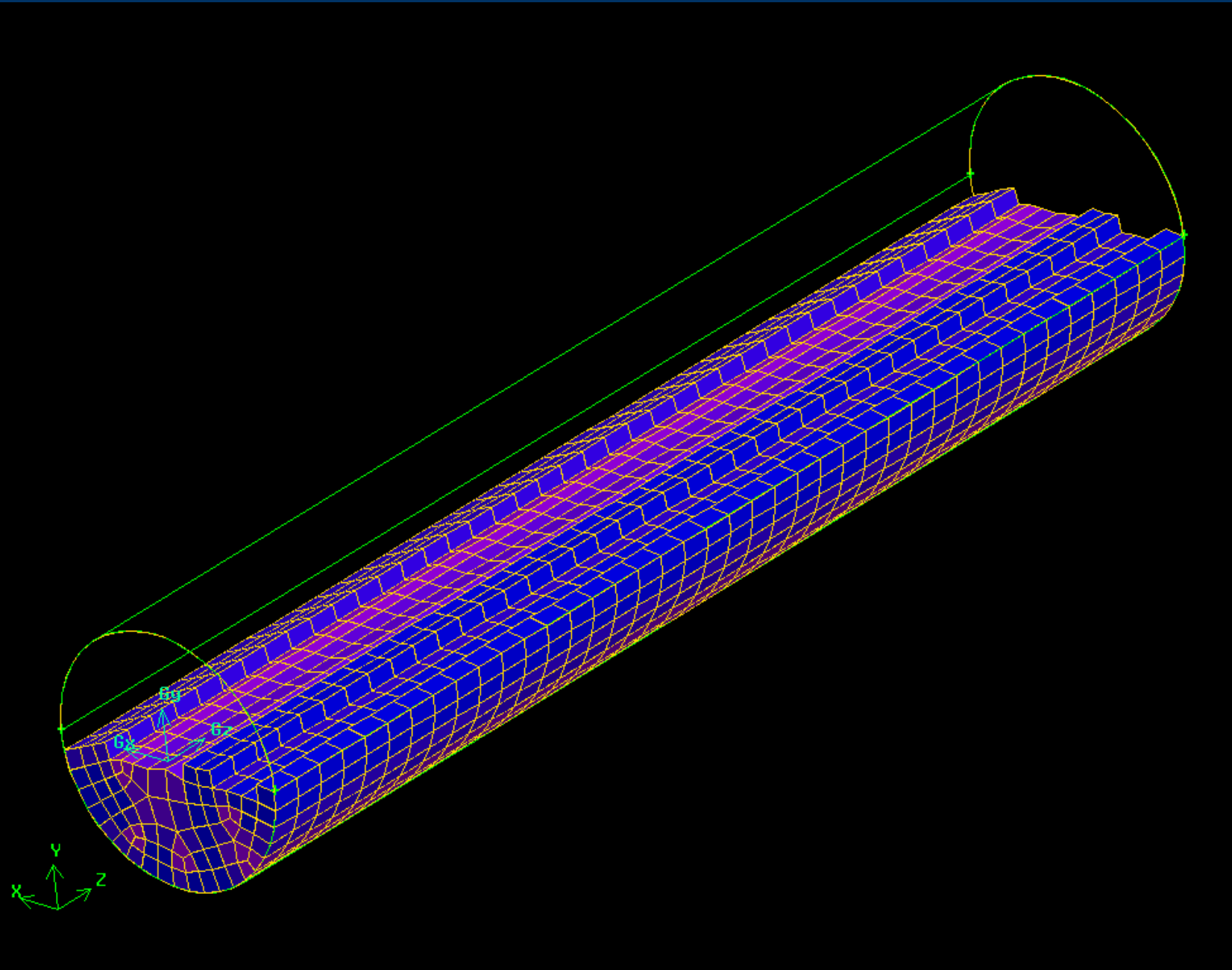


Pipe Mesh Testing



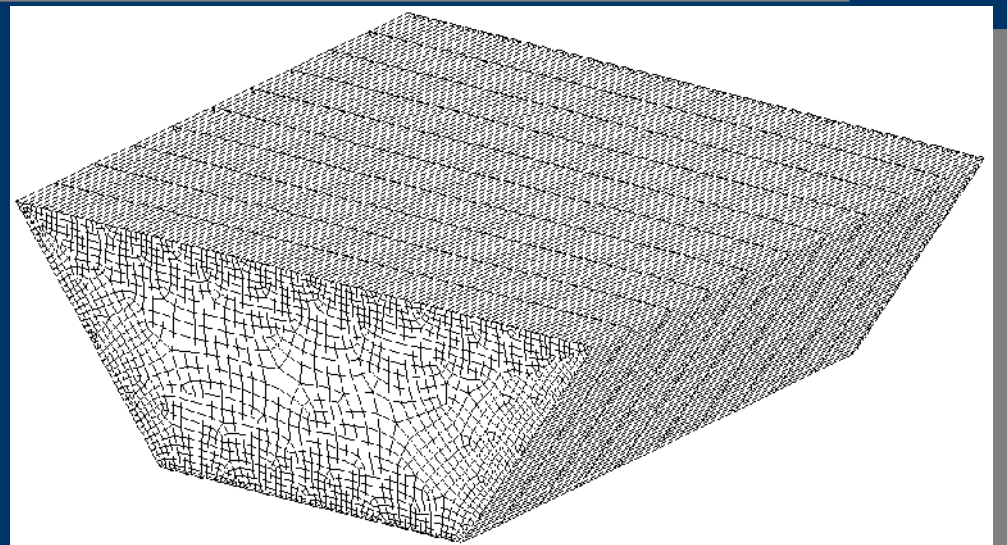
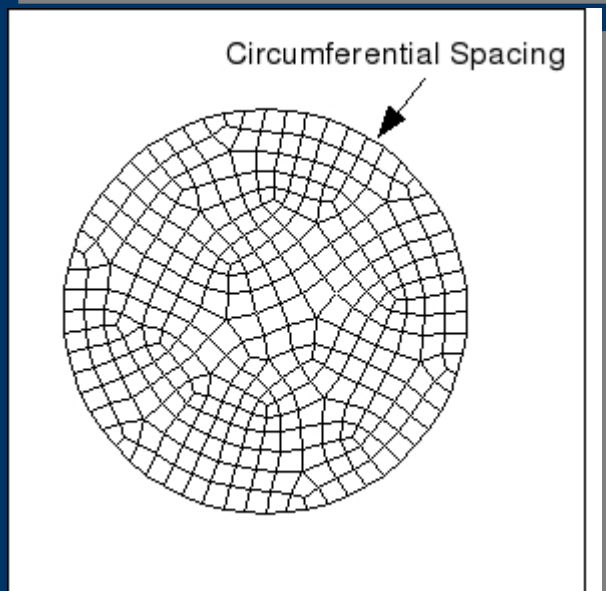
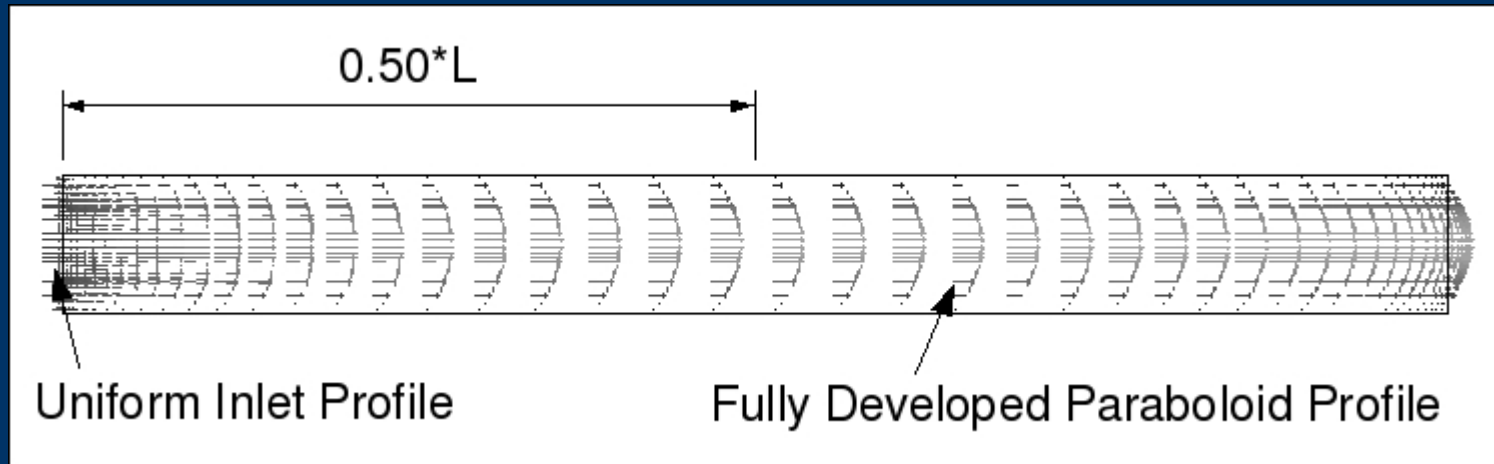
“Bell Shaped” Axial Space

Pipe Mesh Testing

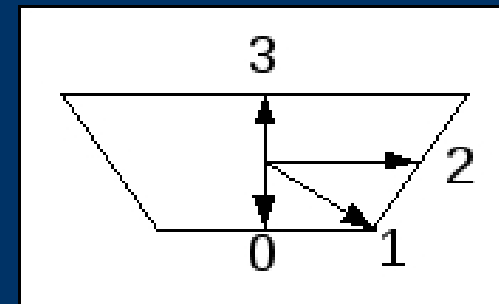
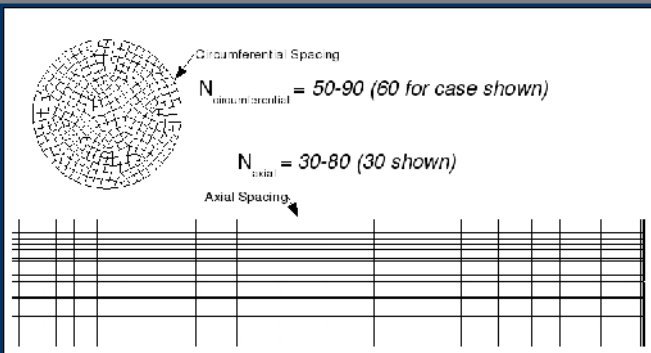
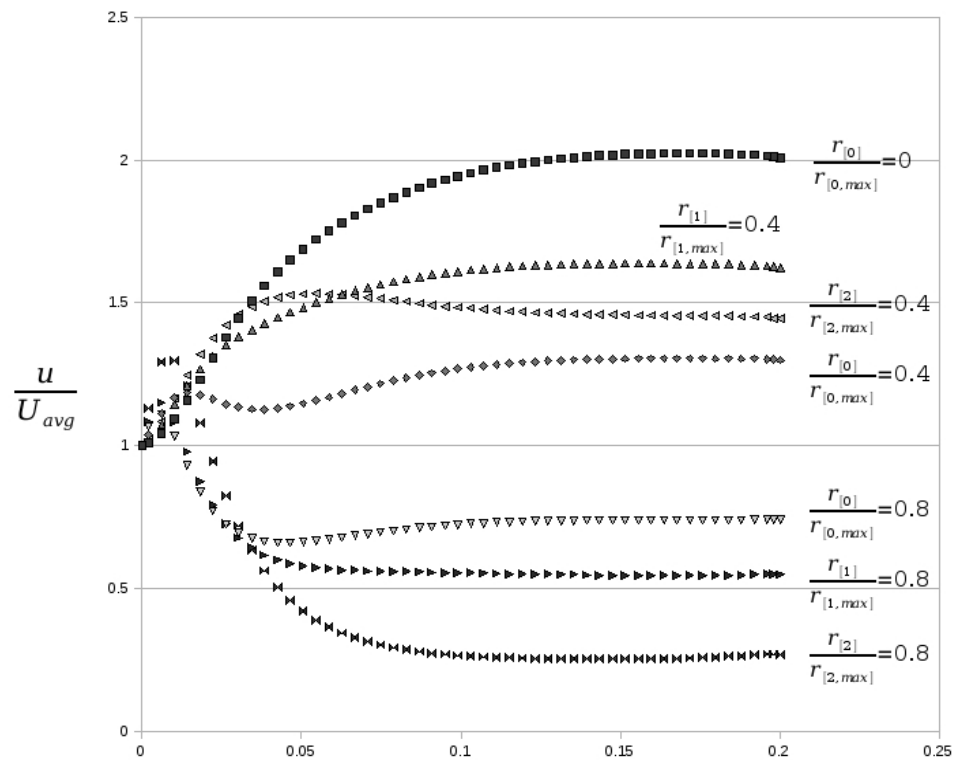
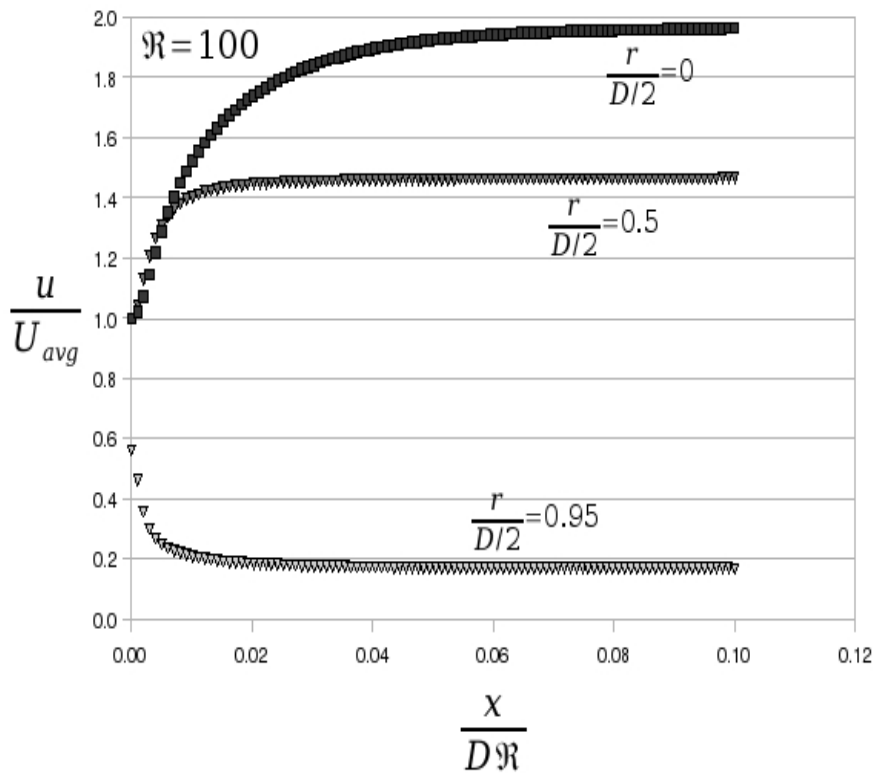


Uniform Axial Spacing

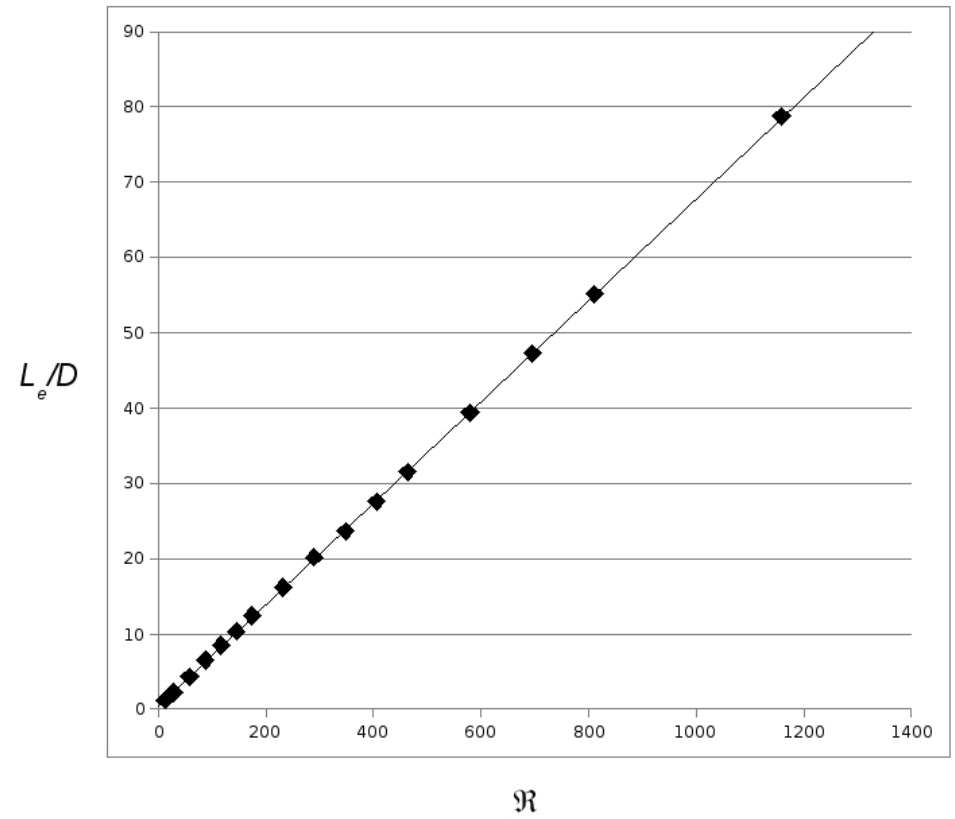
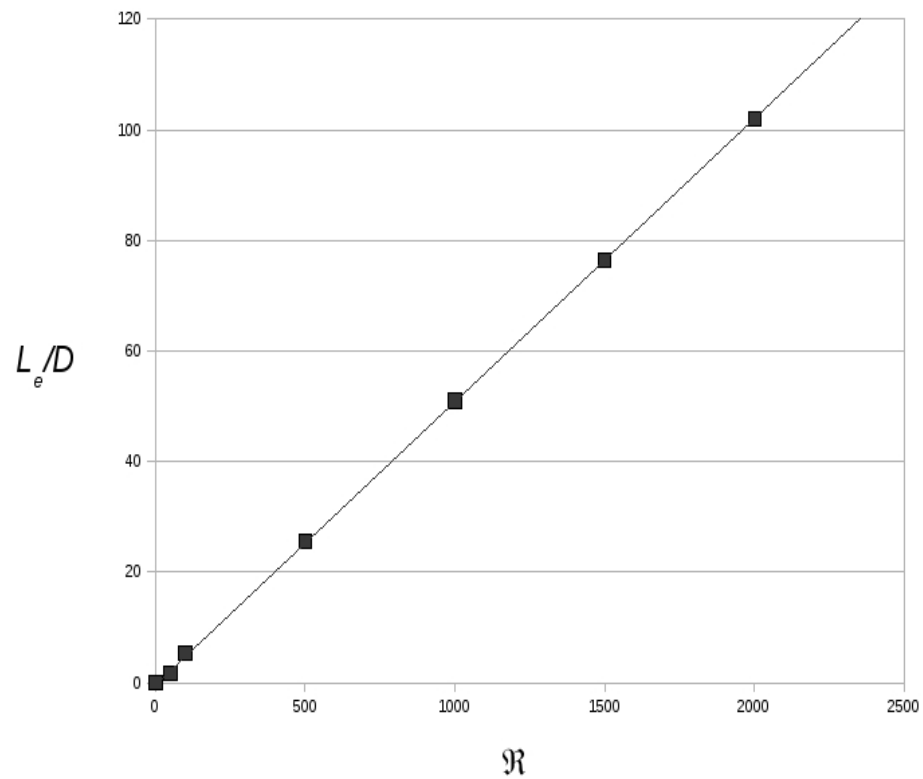
Entrance Length in Microtubes



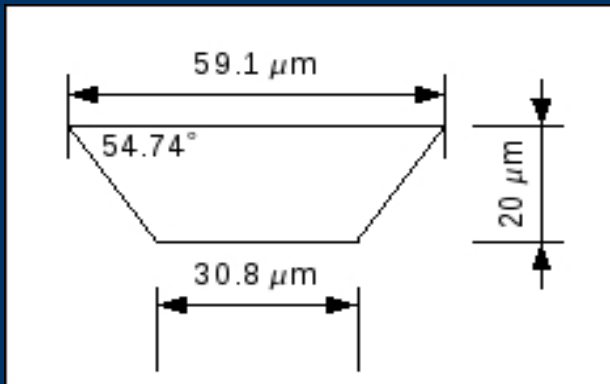
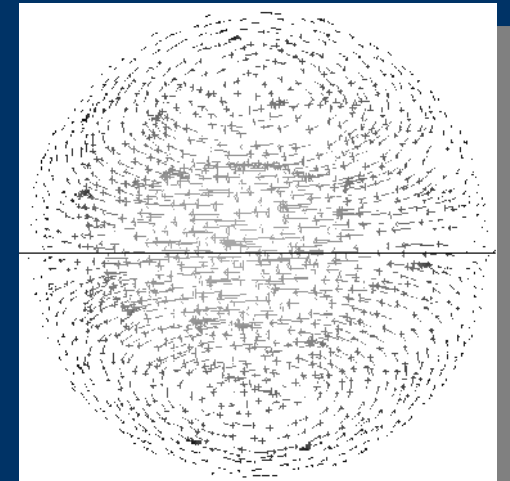
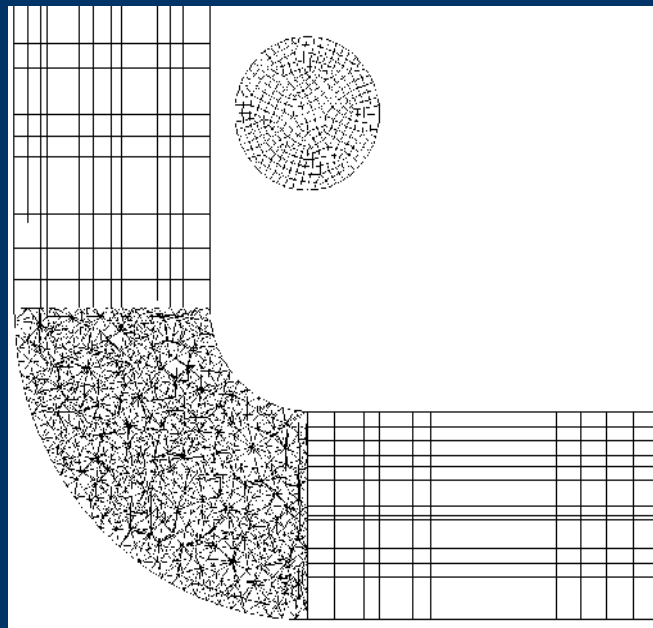
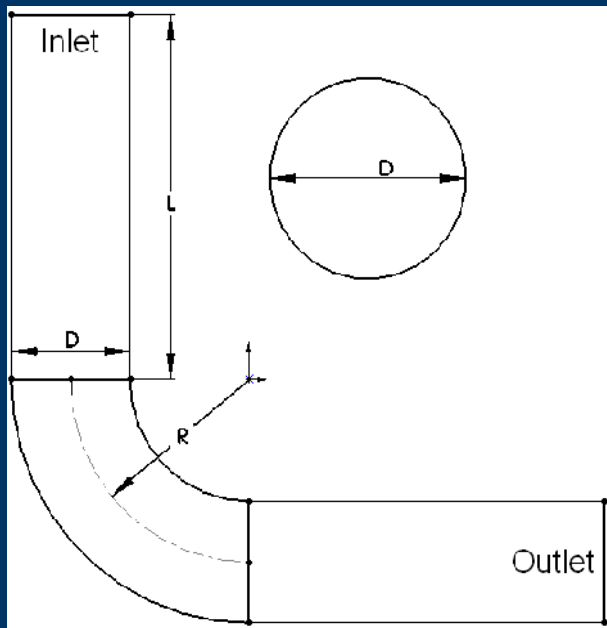
Entrance Length Results



Entrance Length Results



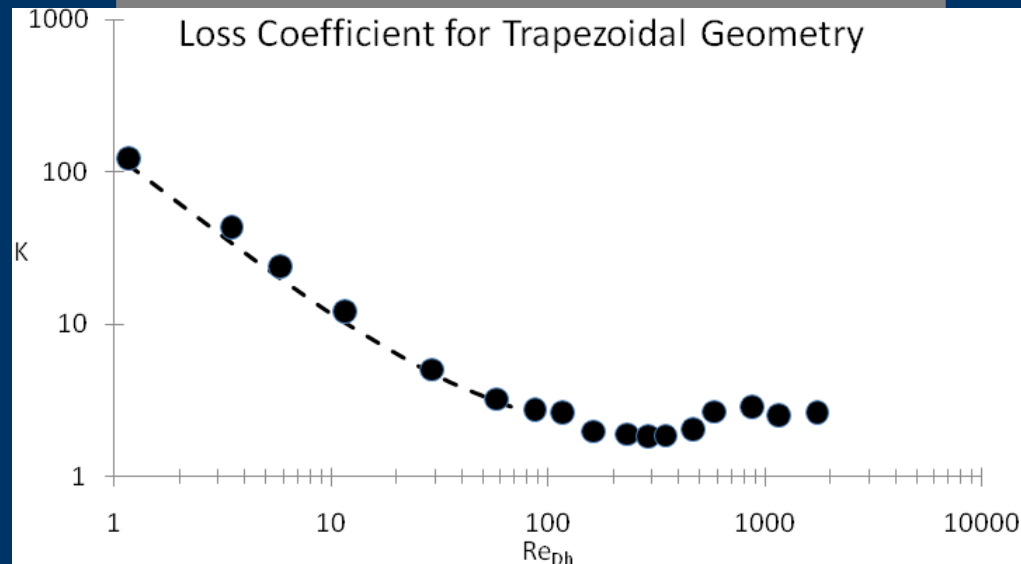
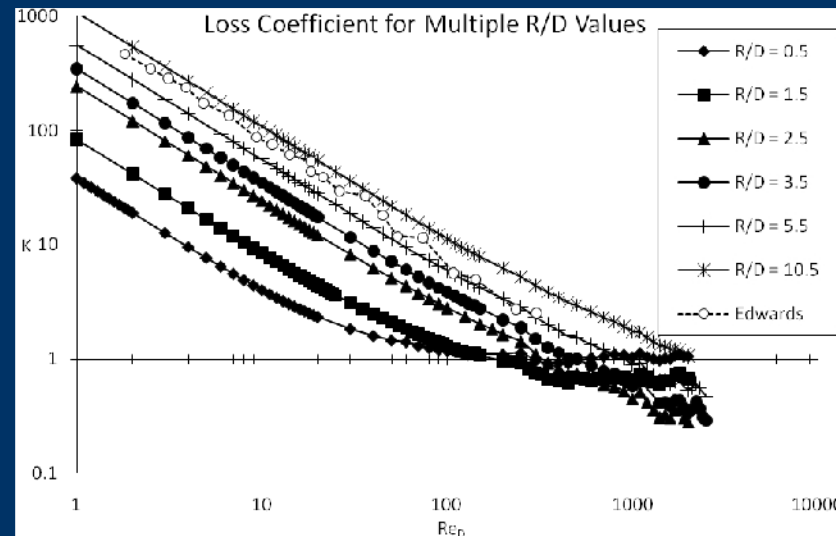
Loss Coefficients in Microelbows



$$K = \frac{\Delta p}{\frac{1}{2} \rho V^2}$$

Microelbow Loss Coefficients

$$K = \frac{\Delta p}{\frac{1}{2} \rho V^2}$$



Millijunction Experiments



DESIGN & PRODUCTION

Objectives:

- ✓ Design improved sealing method for part and increase re-usability of parts
- ✓ Test the new designs
- ✓ Document the production process

New Seal Design

We needed a seal design that would be leak-free and allow for quick and easy assembly and re-usability. The chosen design is loosely based on fuel injector seals.



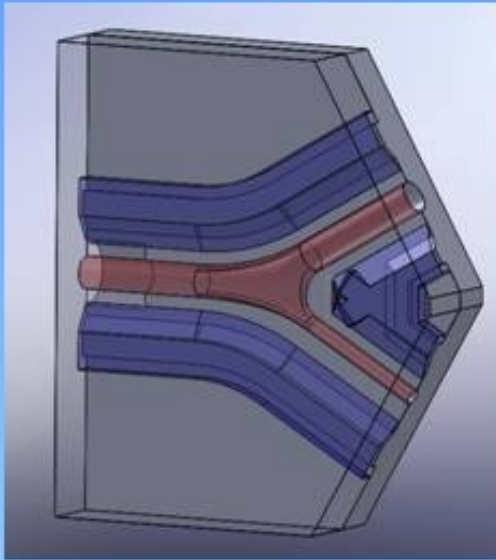
Two o' rings are placed on the ends of each connecting pipe downstream from the head tank.



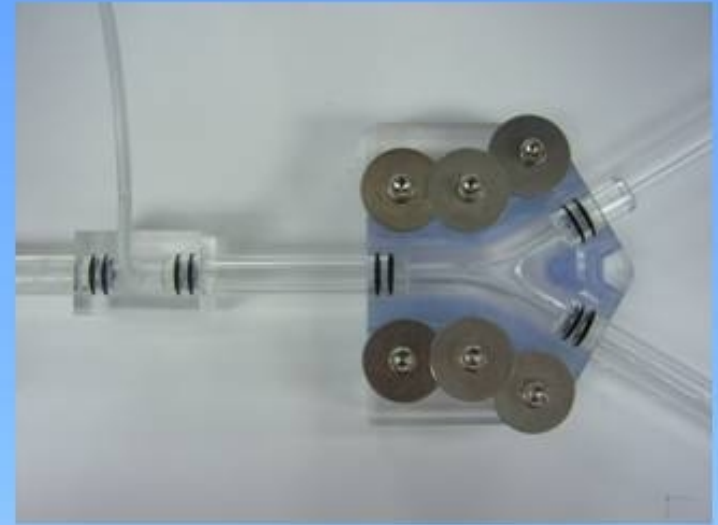
New tap blocks were milled to allow for flexibility in pressure tap placement. By adapting the smaller OD tubing to $\frac{1}{2}$ " we can use one block design for multiple sizes of tubing. The left is the inlet block and the right is the $\frac{1}{8}$ " outlet.

The existing flow straightener was reused by manufacturing an adapter that converted the threaded end to the new o'ring type. This design has the advantage that there is no time spent waiting for sealant to dry so parts can be swapped out with no down time.





Here is the Solidworks model as well as the physical realization of our efforts to create a useable bifurcation.



Upstream from the head tank and downstream from the junction are our new, highly sensitive needle valves used to adjust the head tank flow and the flow fraction through the bifurcation.



The flow straightener we designed has a replaceable core made of glass micropipettes that can be removed completely for unrestricted flow.



Data Acquisition

Jesse Haubrich

Collecting Data

Sensor

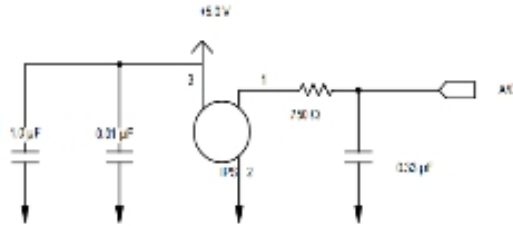
- Submersible
- Internal Instrumentation Op-Amp



MPVZ5004GW7U
CASE 1560-02

Filter

- 750Hz Low Pass
- Reduces Noise from 10mV to 2mV



ADC

- 12 bit
- 11 Channel



Basic Stamp

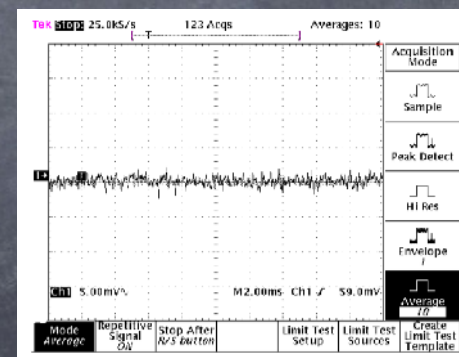
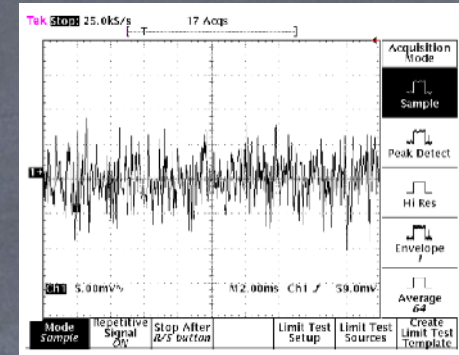
- Easy to program
- Affordable



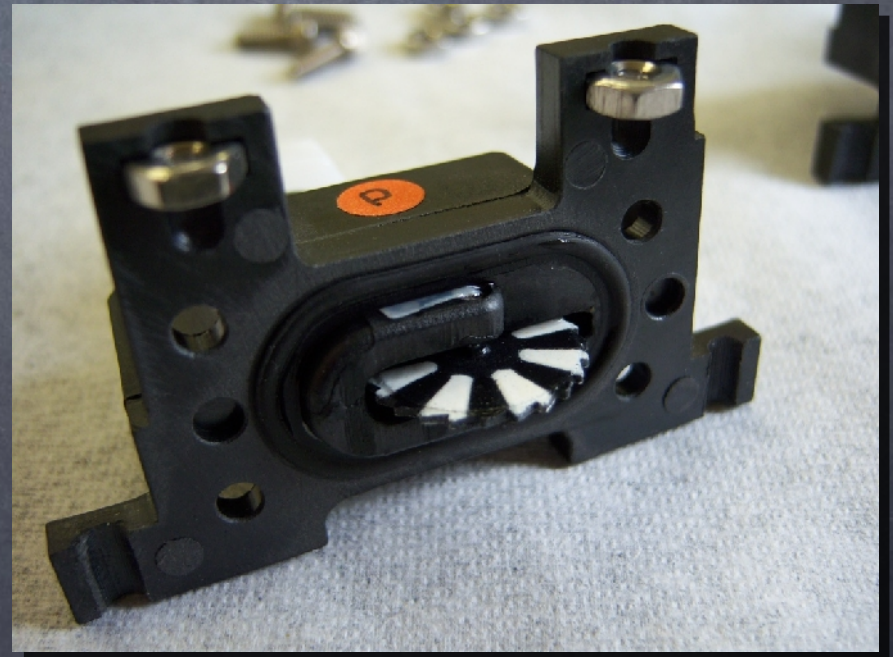
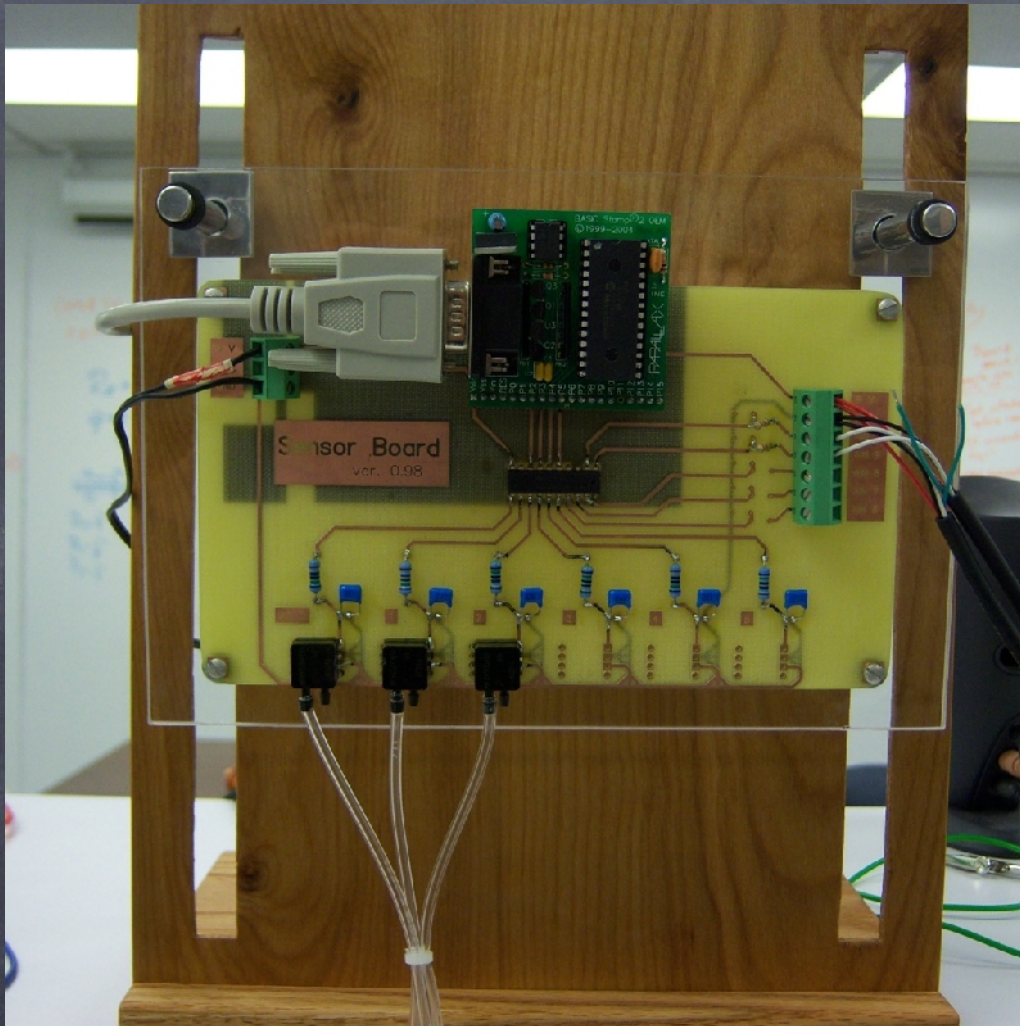
Computer

- Python
- Real Time Plotting with GNU Plot

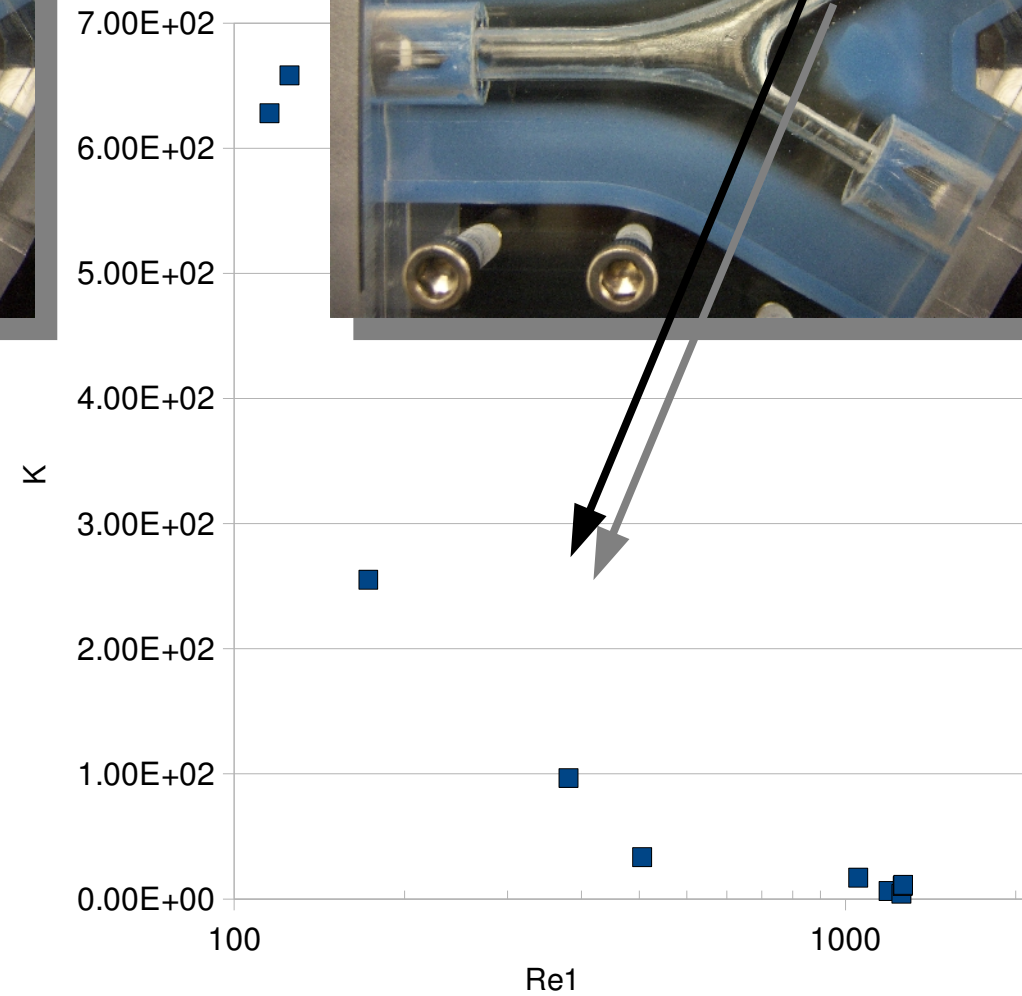
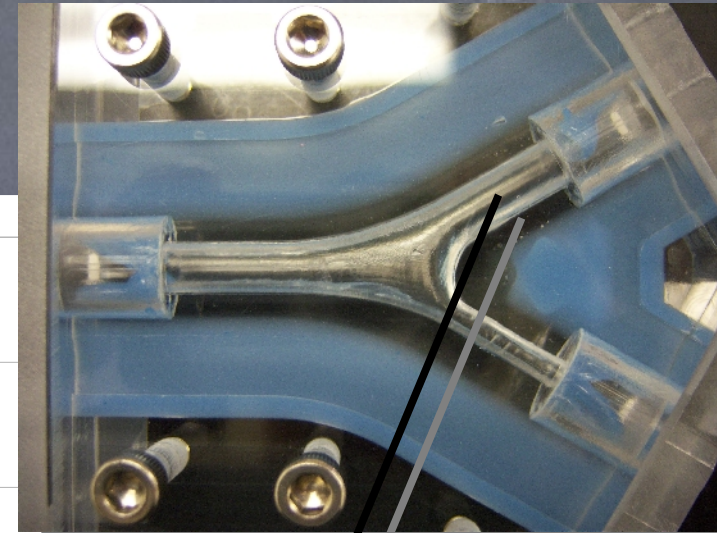
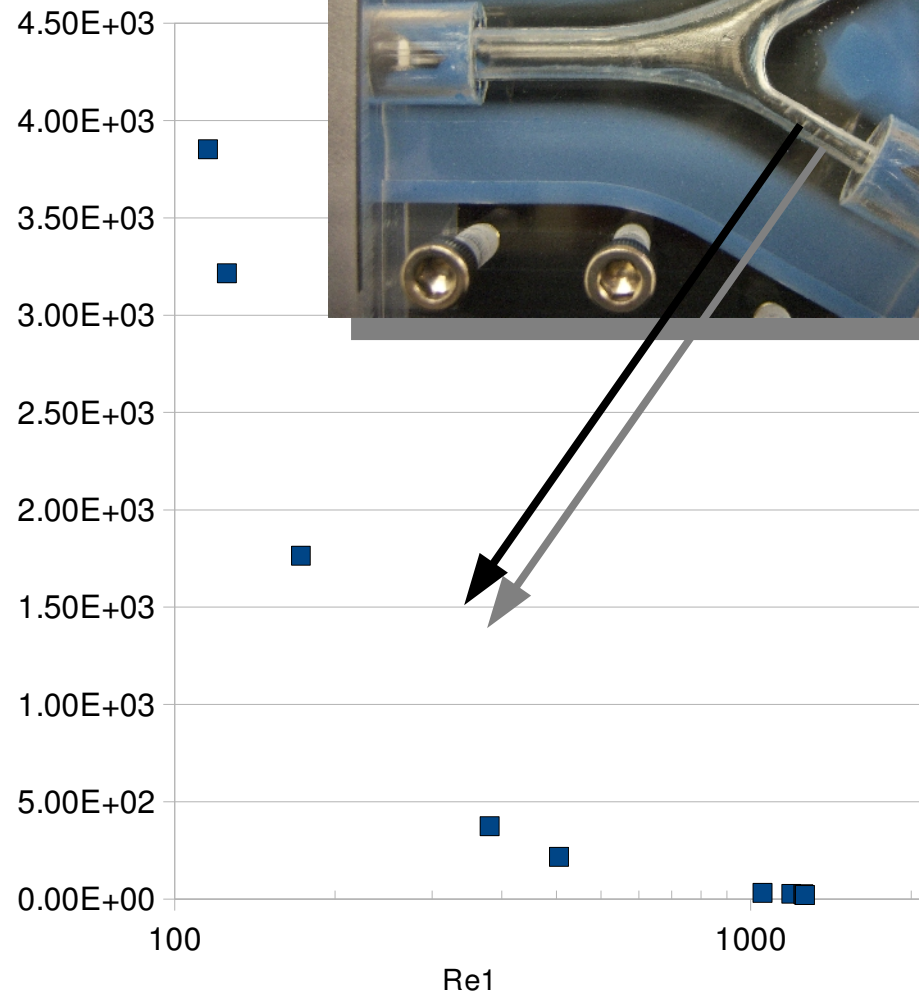
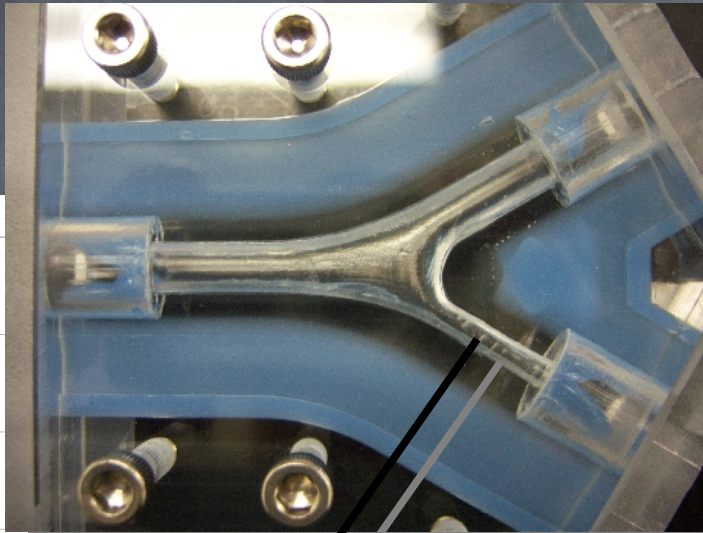
```
if __name__ == '__main__':  
    serial = connect_serial()  
    filesave = csv.writer(open("data.csv", "wb"))  
    while True:  
        data = serial.readline().split()  
        filesave.writerow(data)  
        plot(data)
```



Basic Stamp
Passive Filter
Pressure Sensors
Flow Sensors
Python Interface



Loss Coefficient Experimental Results



Using Network Simulations to Understand Non-Darcy Flow

Objectives

Develop an algorithm to create, mesh, and perform CFD on simplified models of real porous media networks.

Equal number of entry and exit pores (no splits)

90° elbows only

No overlap of pores within media

Compare results of CFD to FTPM and empirical data in literature.

Modify algorithm to allow for complex models of real porous media.

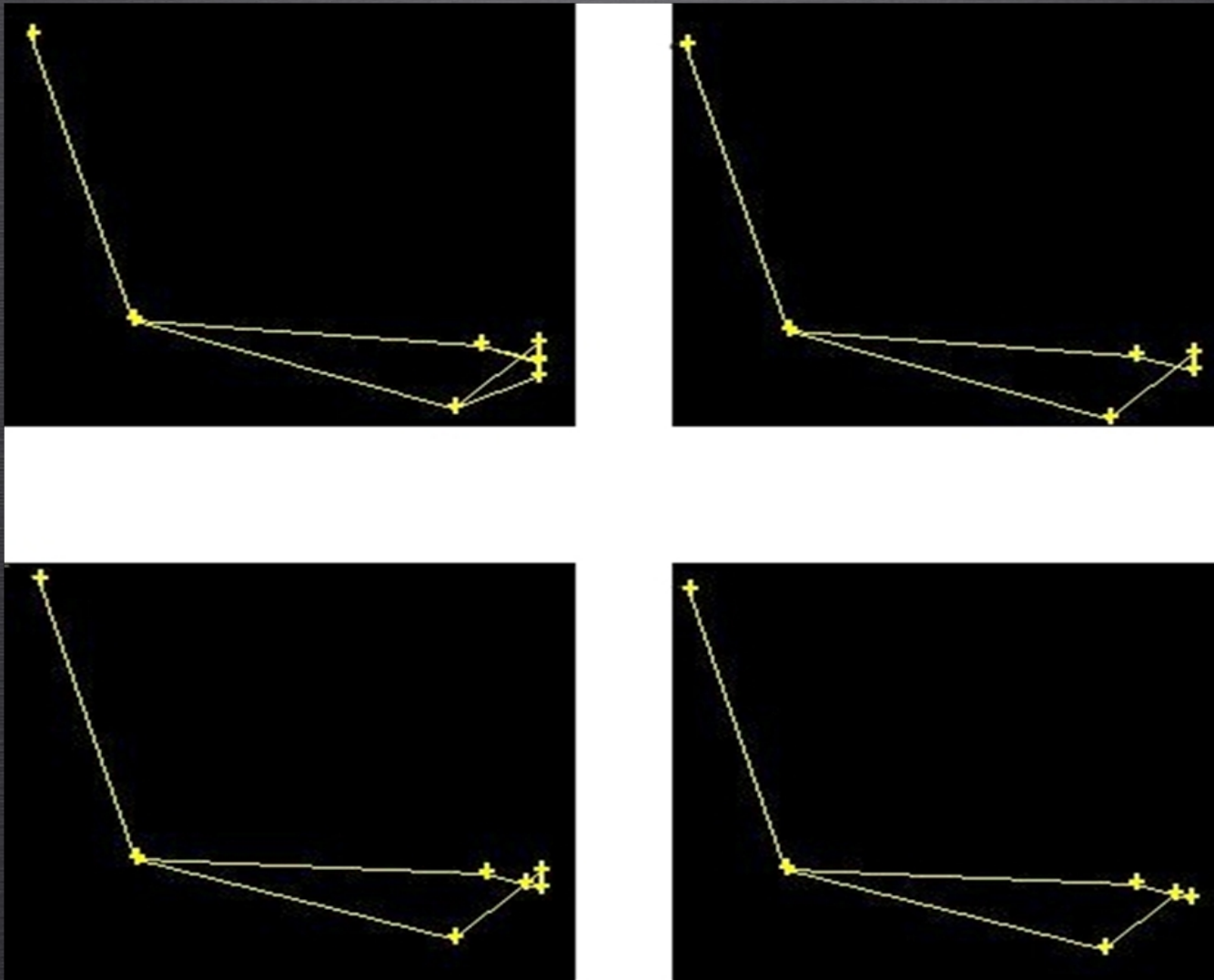
Splits with arbitrary angles

Overlaps

Using Network Simulations to Understand Non-Darcy Flow

Implementation of Objectives

Use custom codes to extract FTPM networks from code

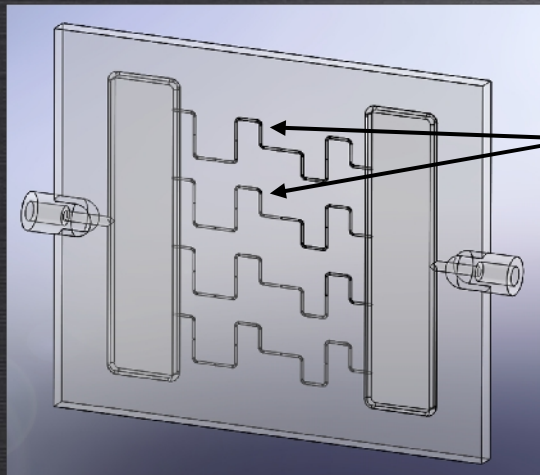


Using Network Simulations to Understand Non-Darcy Flow

Implementation of Objectives

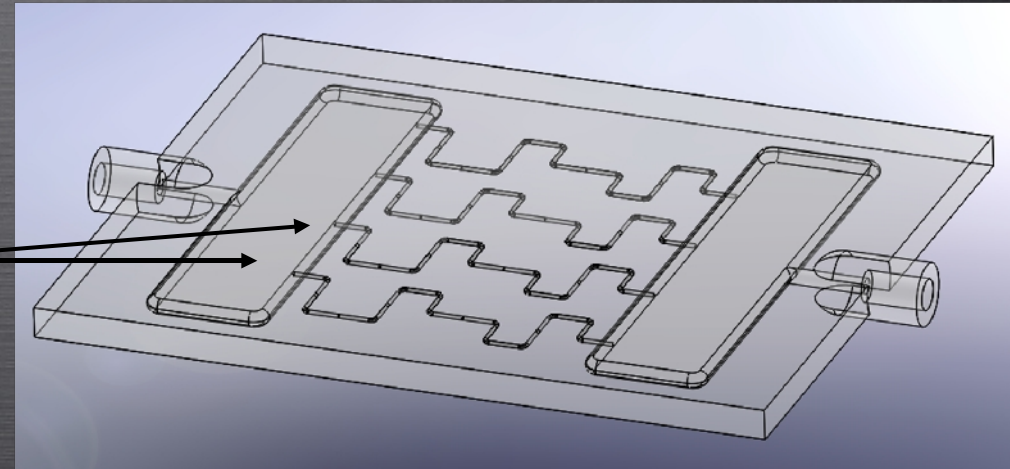
Use Solidworks to create network designs

Phase 1



90° elbows

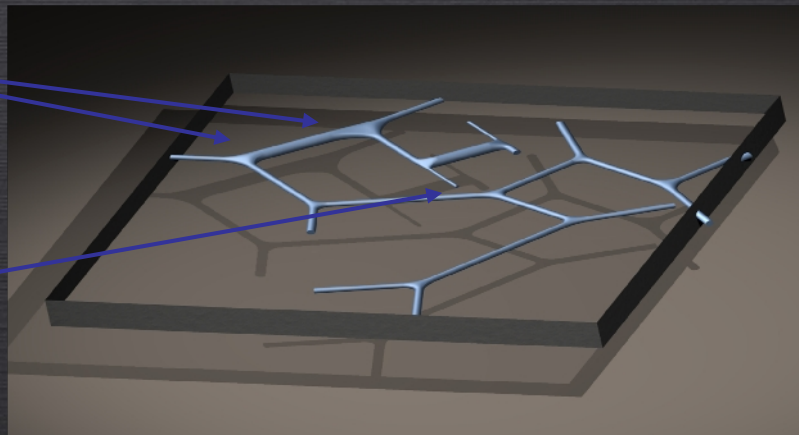
No overlapping



Phase 2

Arbitrary angles

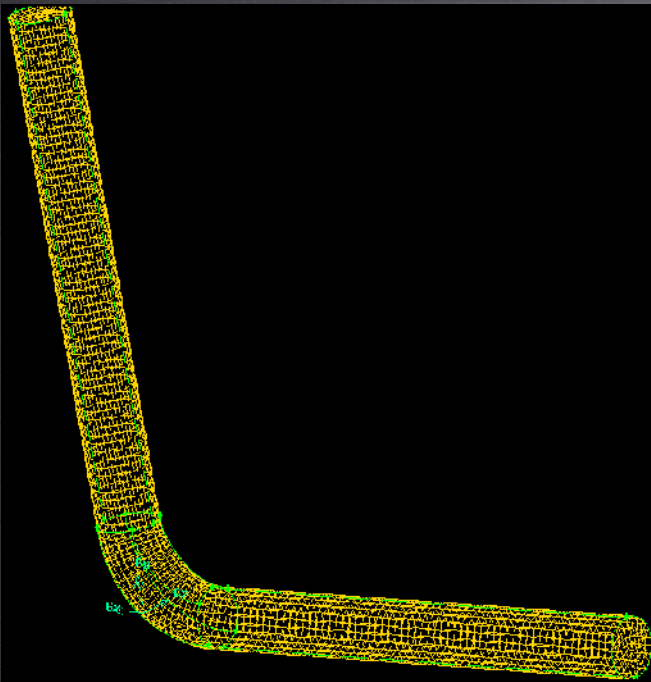
Possible overlaps



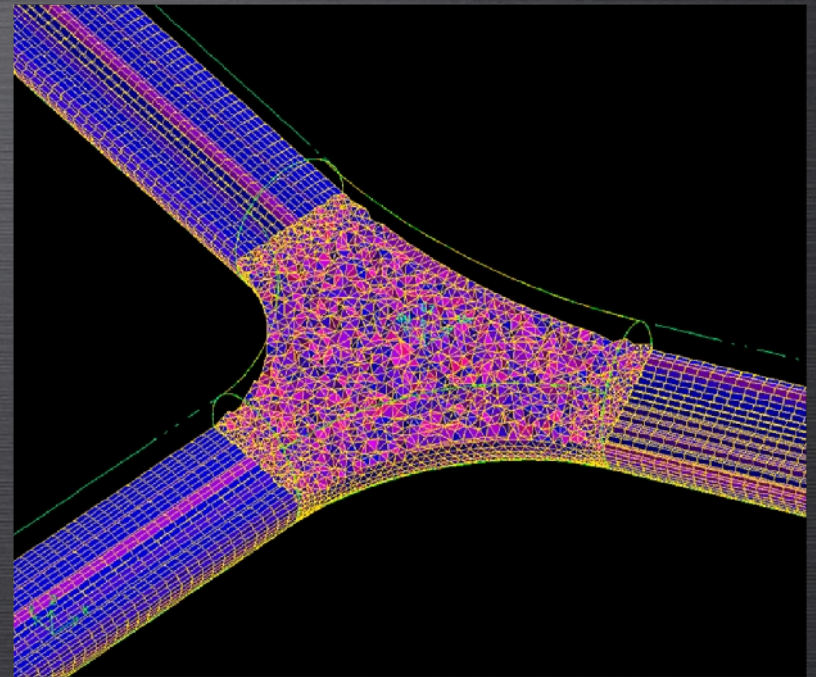
Using Network Simulations to Understand Non-Darcy Flow

Implementation of Objectives

Use Gambit to mesh networks



Close up of 90° elbow

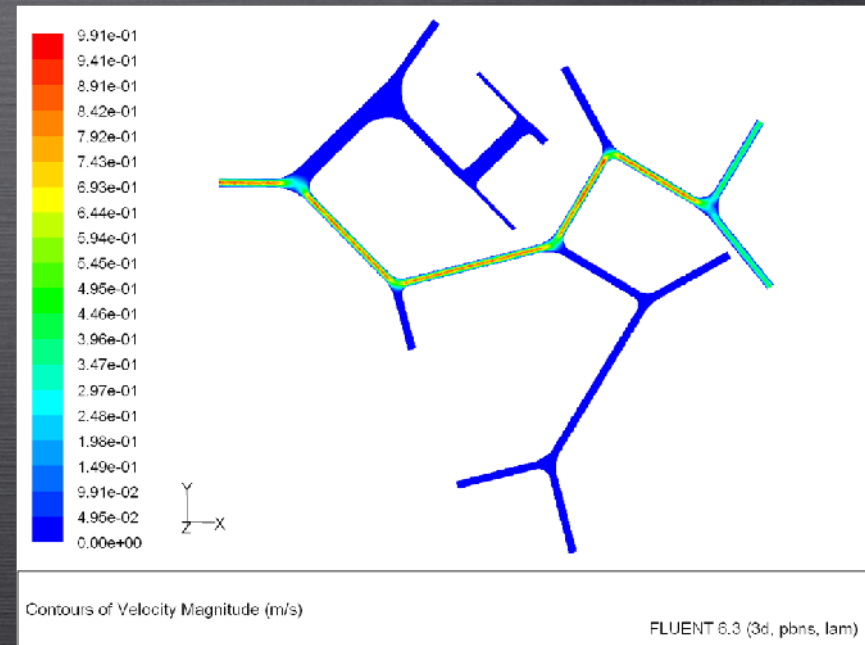
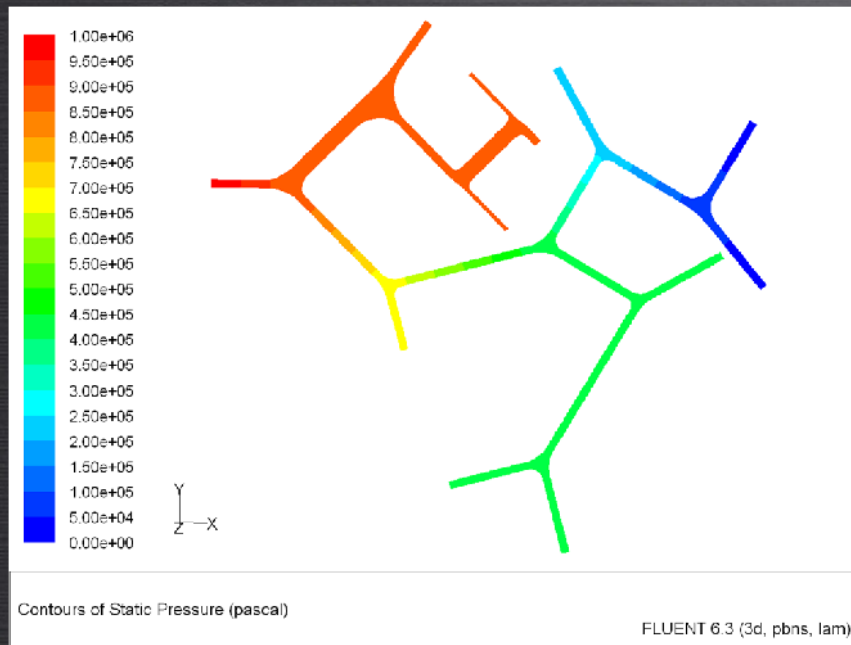


Close up of arbitrary junction

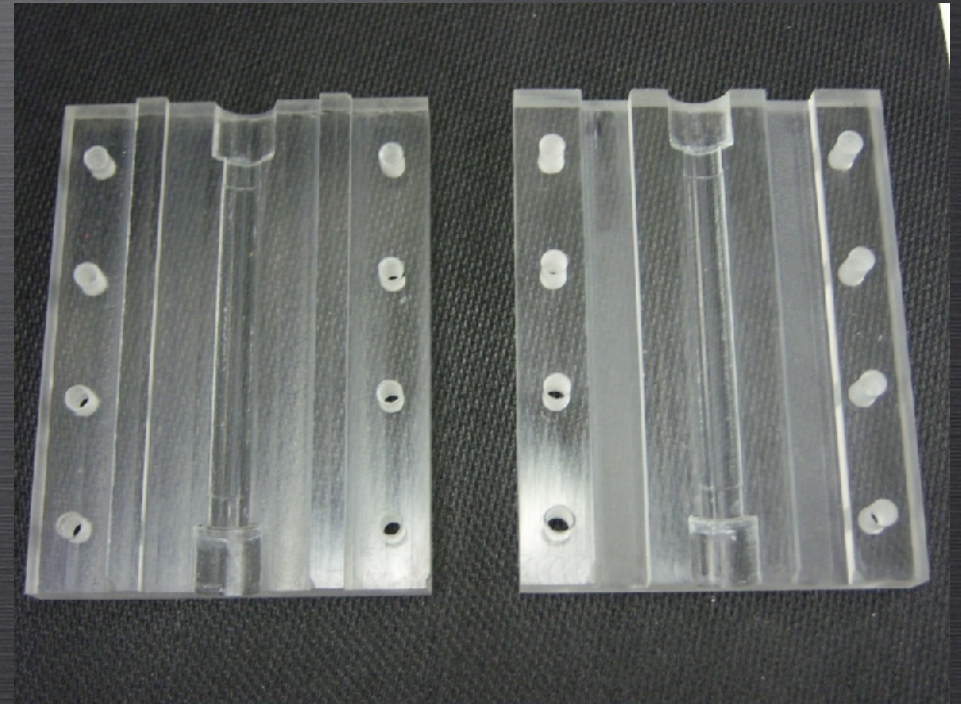
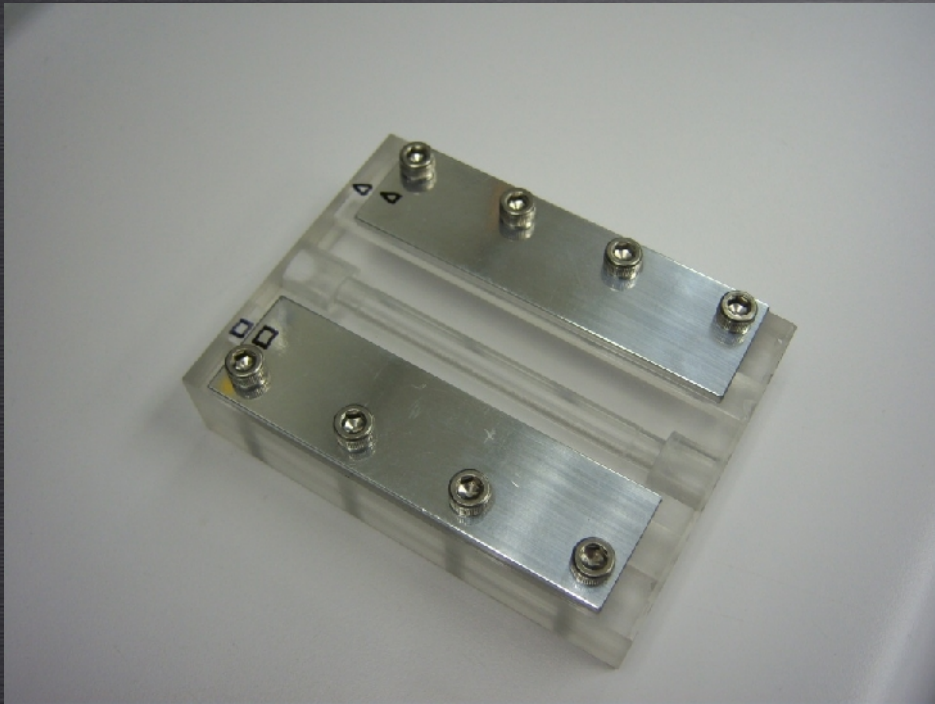
Using Network Simulations to Understand Non-Darcy Flow

Implementation of Objectives

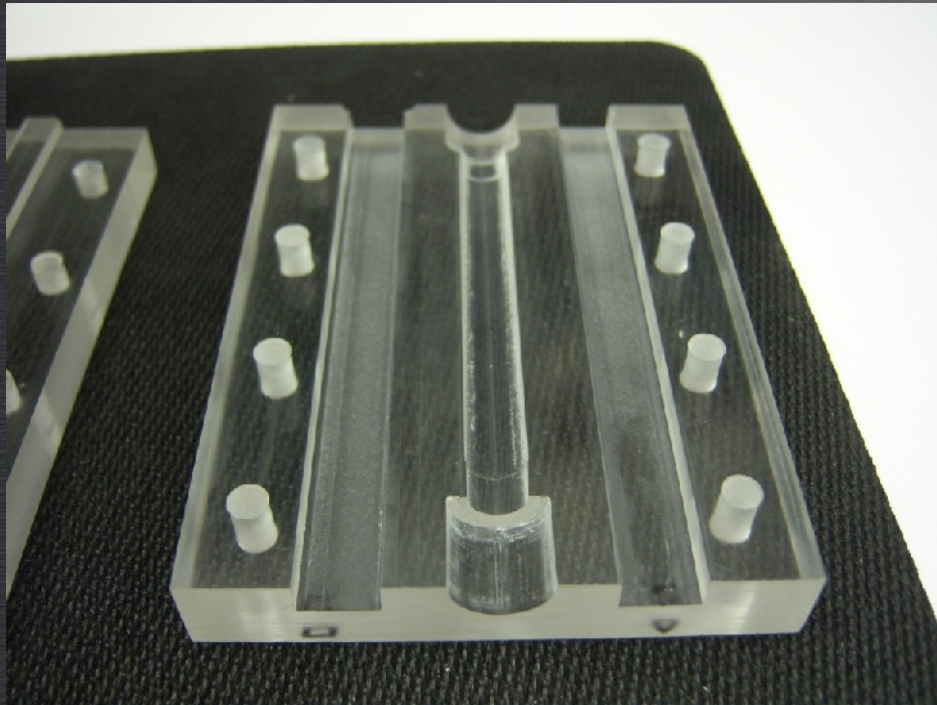
Use Fluent (CFD) to obtain κ and β from pressure and velocity data



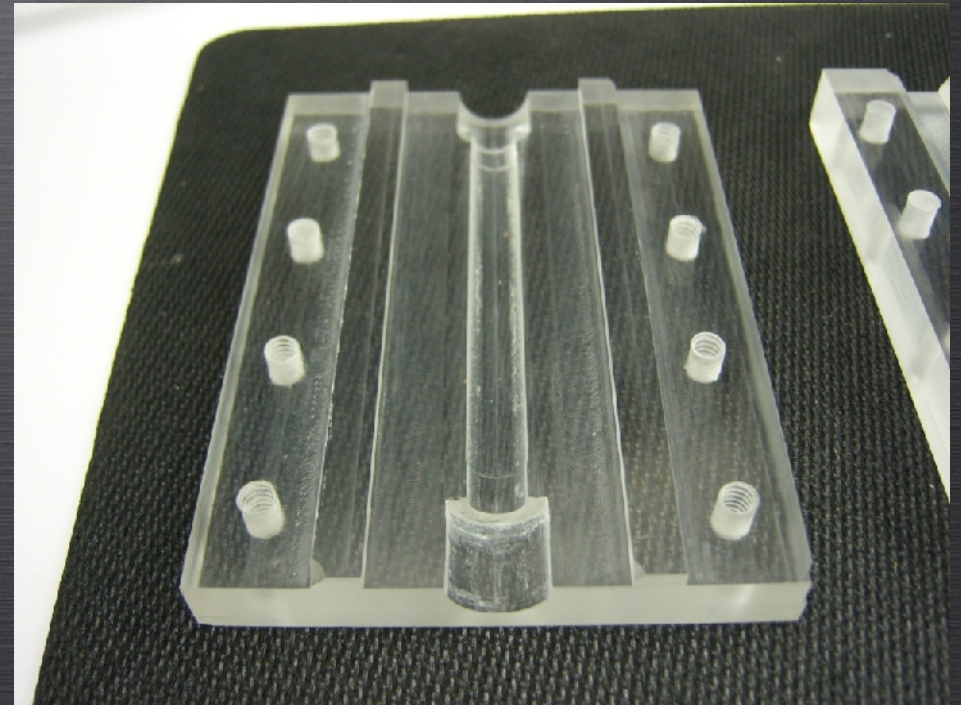
Bio-Scaffold Testing



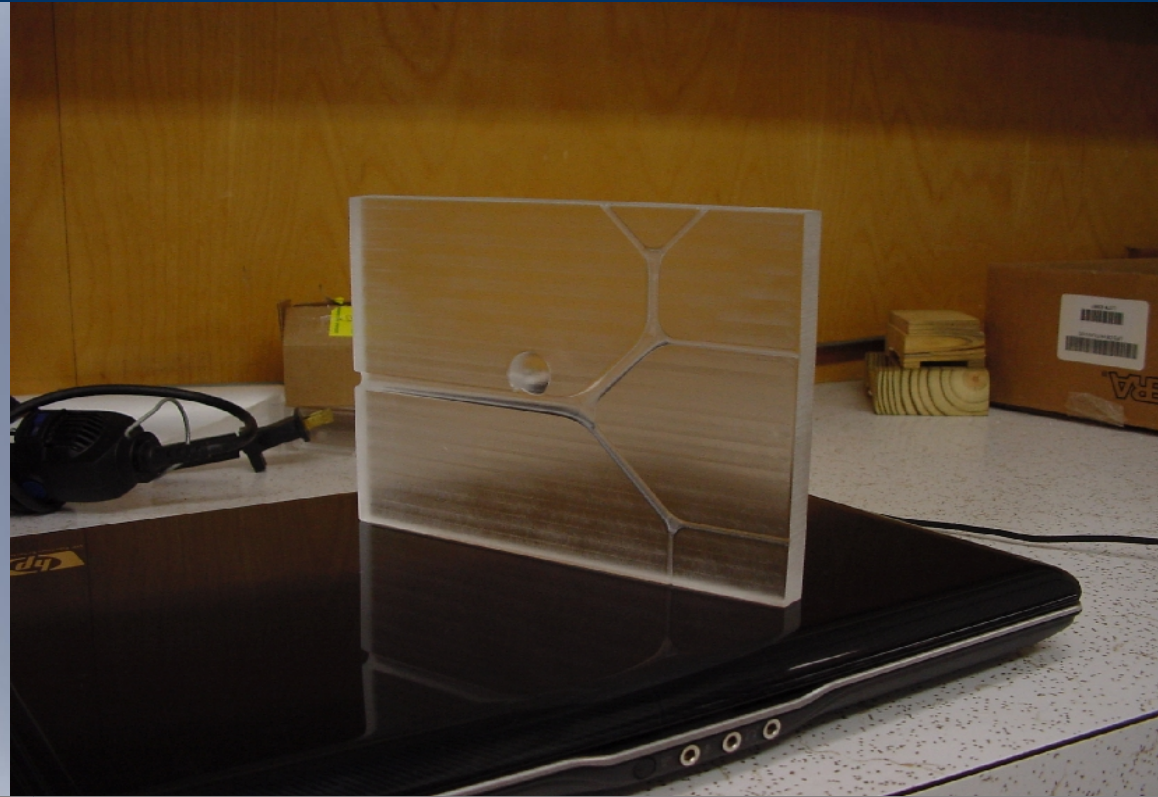
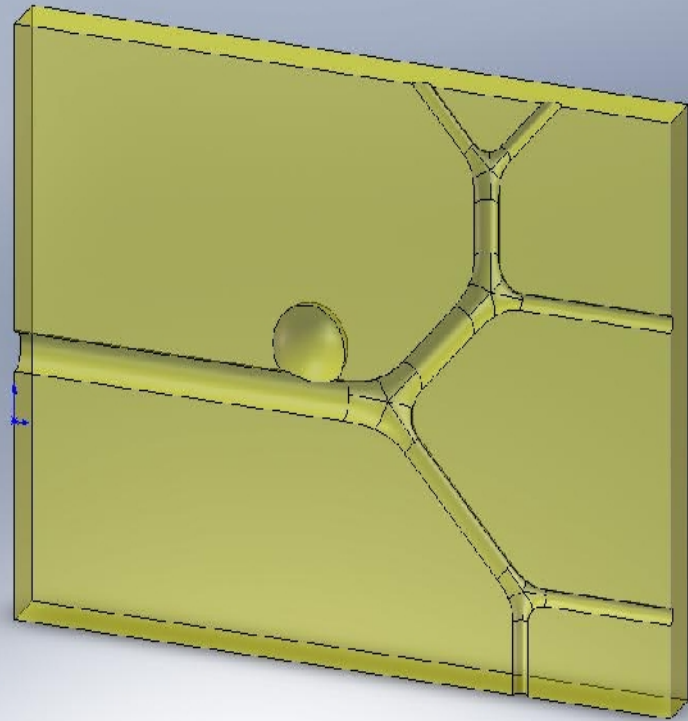
Top



Bottom

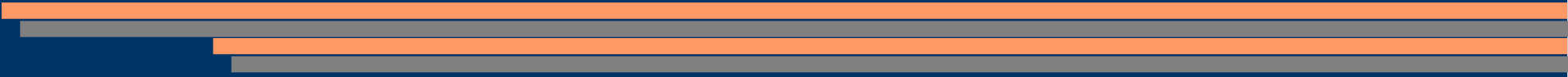


Renal Artery Aneurysm Experiments



Acknowledgments

The Office of Research and Grants at the University of Central Oklahoma is acknowledged for support of this research. The Donors of The Petroleum Research Fund, administered by the American Chemical Society, are also be acknowledged for support of this research through grant PRF# 47193-B9. National Science Foundation EPSCoR Research Opportunity Award Program

The slide features three horizontal bars at the bottom: a thick orange bar, a thin grey bar, and another thick orange bar.